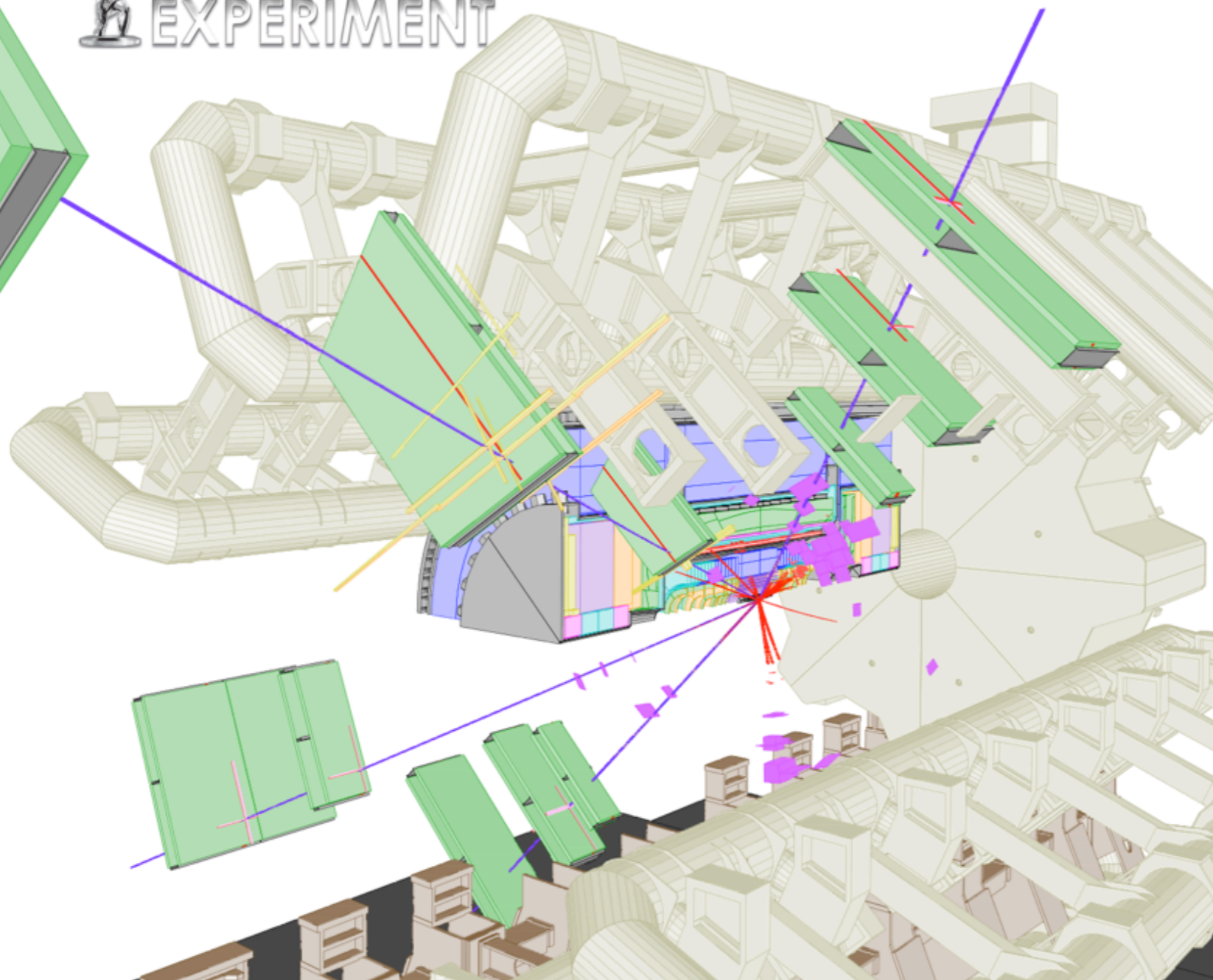


Run Number: 183003,
Event Number: 121099951
Date: 2011-06-02, 10:08:24 CET
EtCut>0.3 GeV
PtCut>2.5 GeV
Cells: Tiles, EMC



PP7 - Higgs Boson Physics

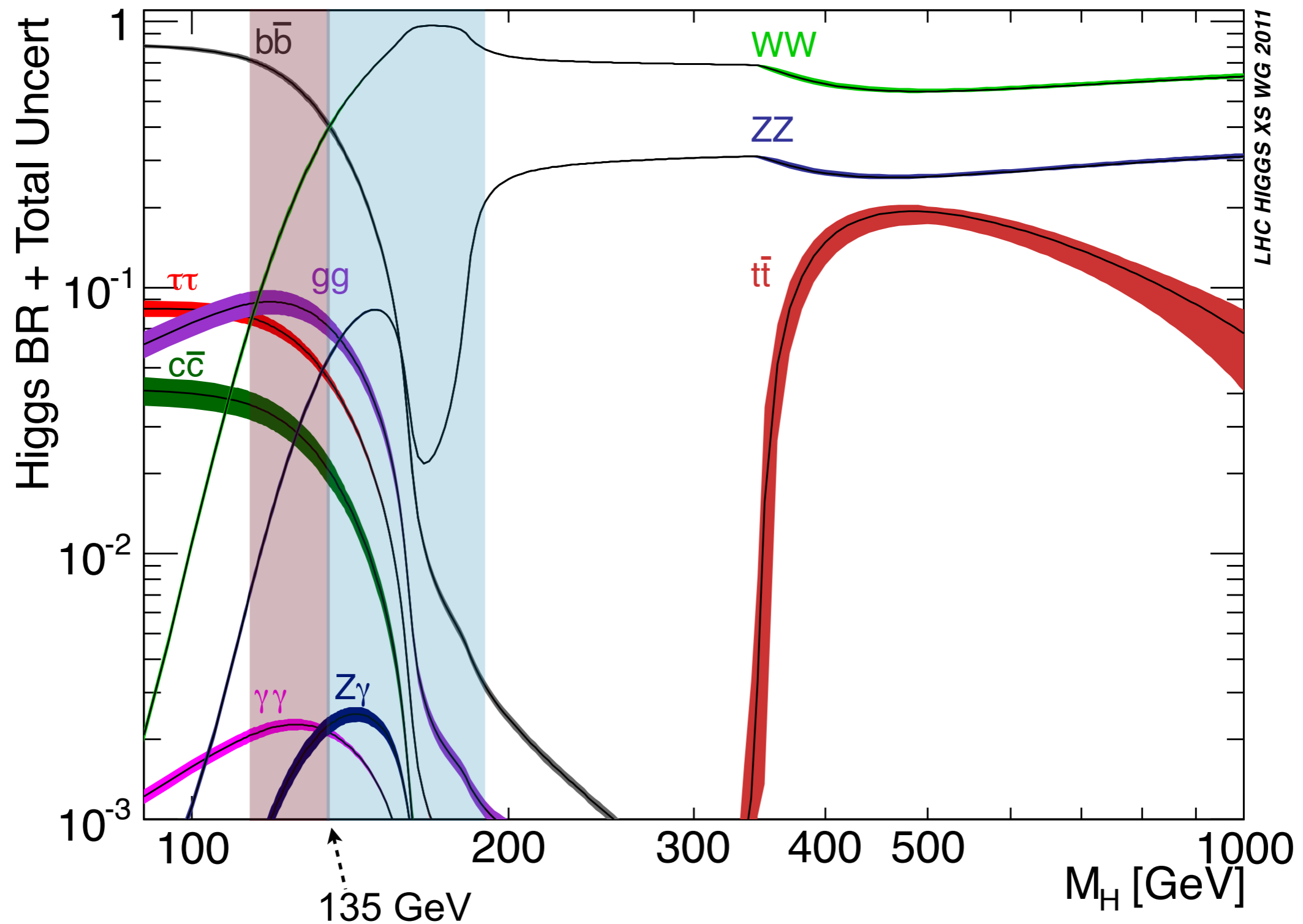
K. Nikolopoulos
University of Birmingham

MPAGS
January, 2014



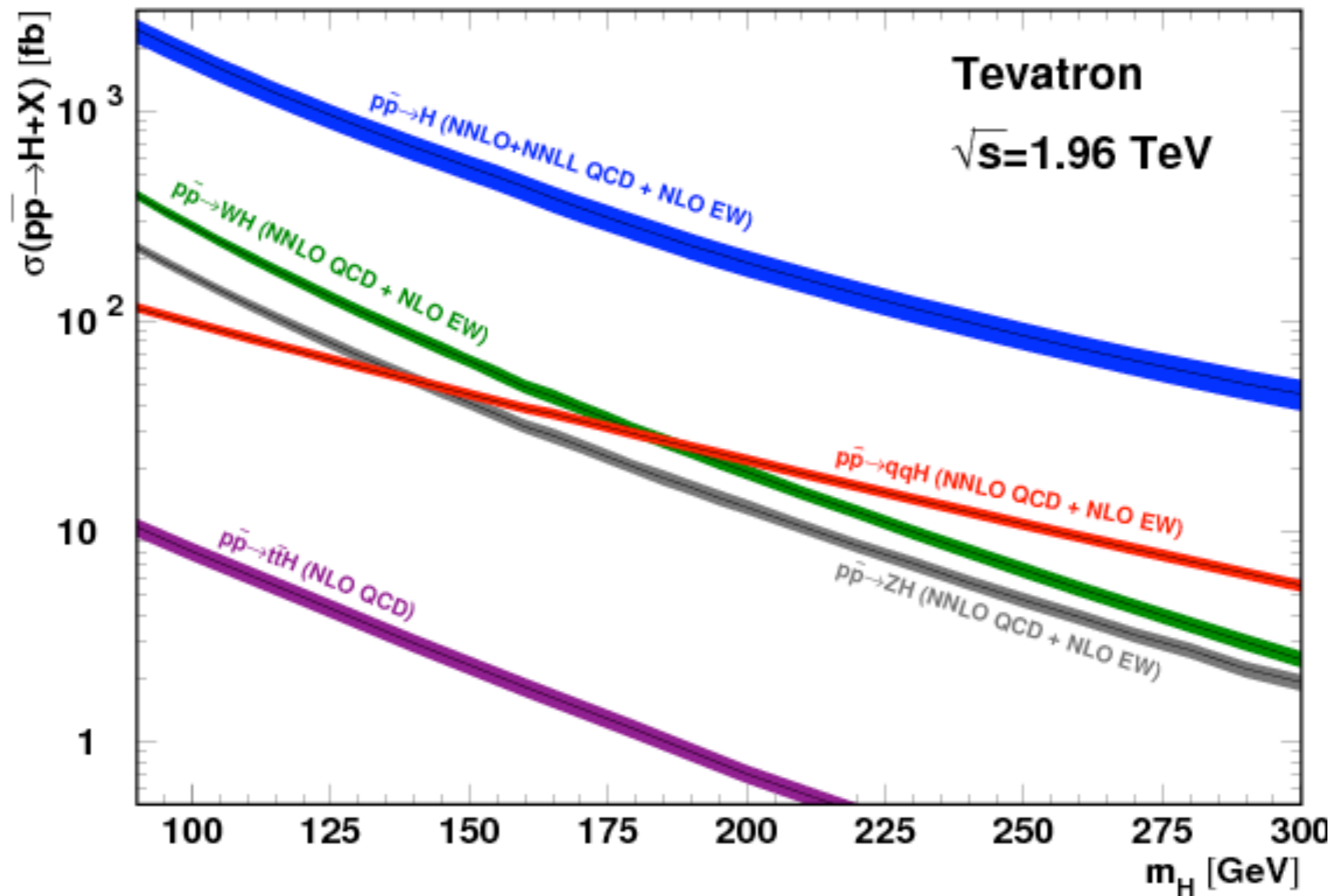
UNIVERSITY OF
BIRMINGHAM

SM Higgs boson decays



Higgs boson is rather short-lived, decaying through different channels!
Following the results from the LEP experiments, TeVatron had to focus in the region with $m_H > 114 \text{ GeV}$

Higgs Boson production at the Tevatron



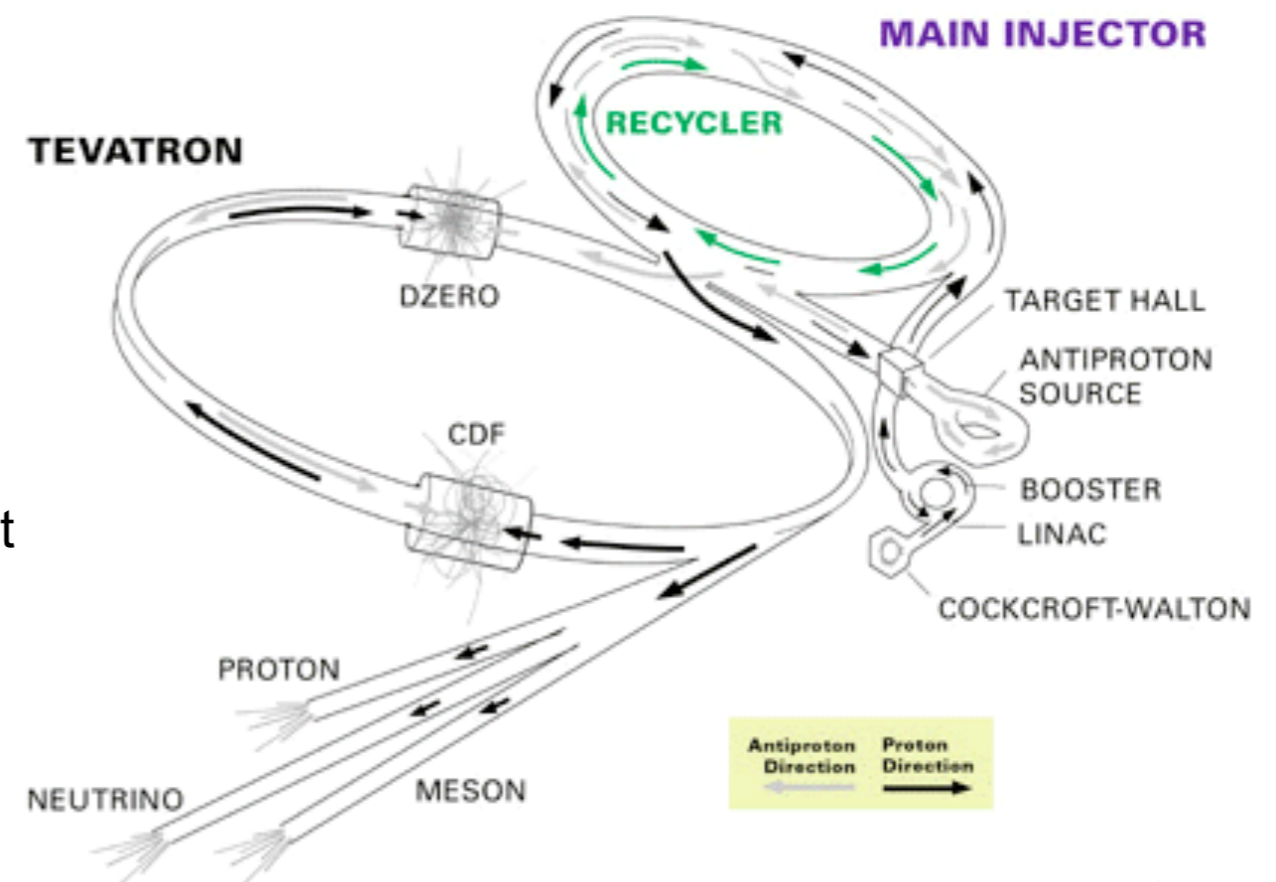
For $m_H < 135$ GeV the decay $H \rightarrow b\bar{b}$ dominates, while $m_H > 135$ GeV the decay $H \rightarrow W^+W^-$ dominates. The former can only be used in the associated production, while the $H \rightarrow W^+W^- \rightarrow l\nu l\nu$ can be used also inclusively

The TeVatron ppbar collider



1985 first proton-antiproton collisions
1988-89 first physics run, CDF
1992-96 Run 1: 120 pb^{-1} , 1.8 TeV, CDF and DØ
1996-2001 Major detector upgrades
2001-11 Run 2: 10 fb^{-1} , 1.96 TeV

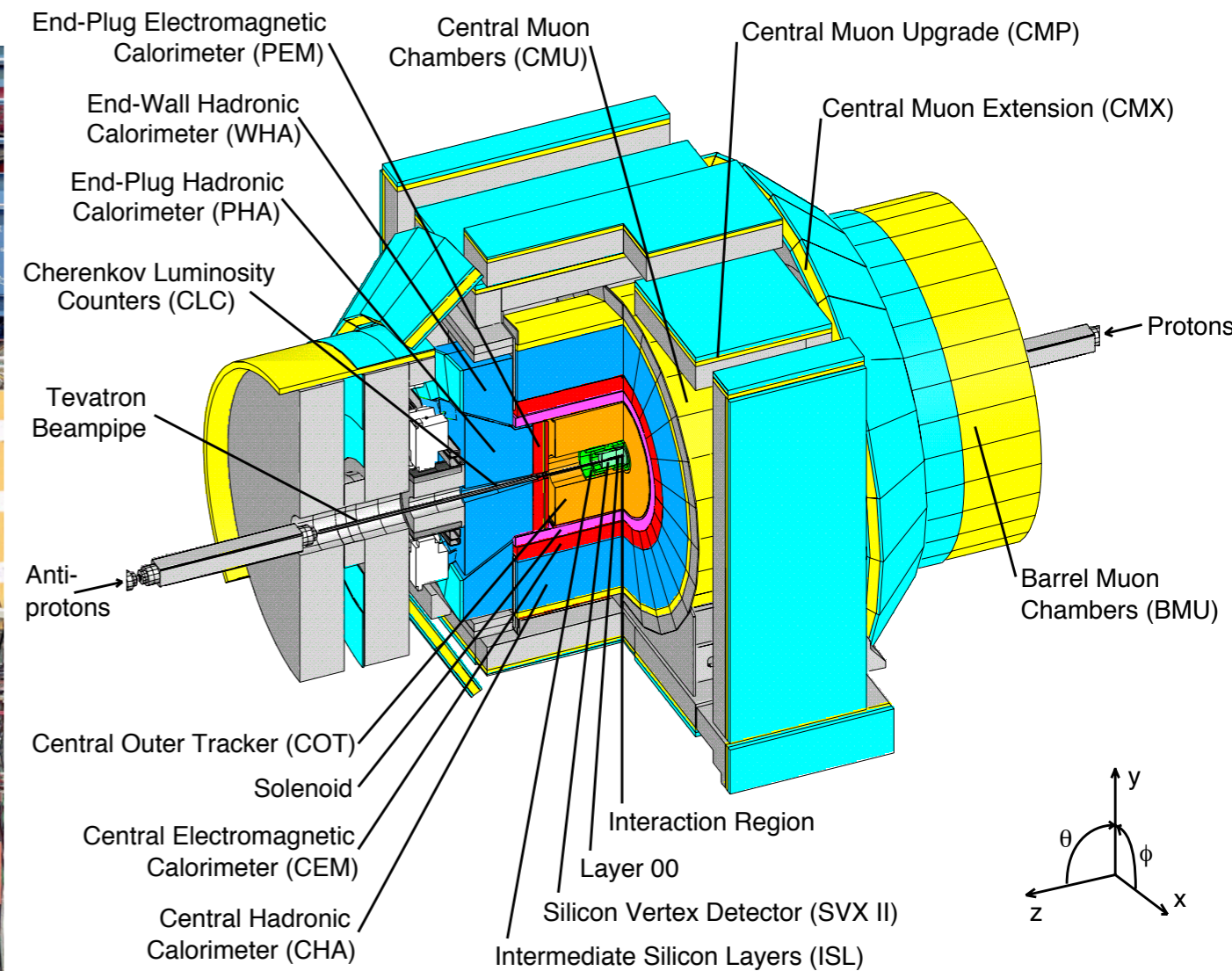
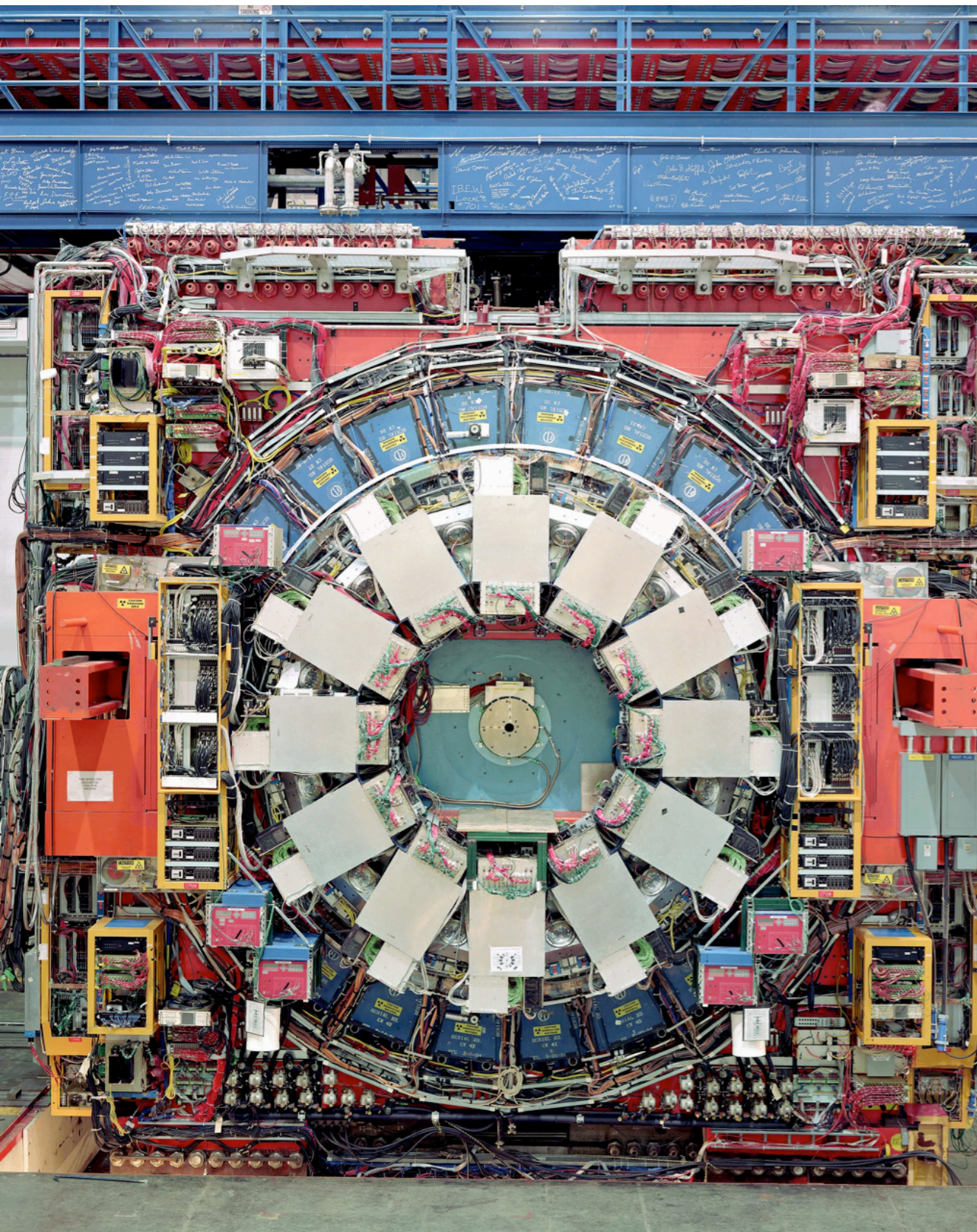
FERMILAB'S ACCELERATOR CHAIN



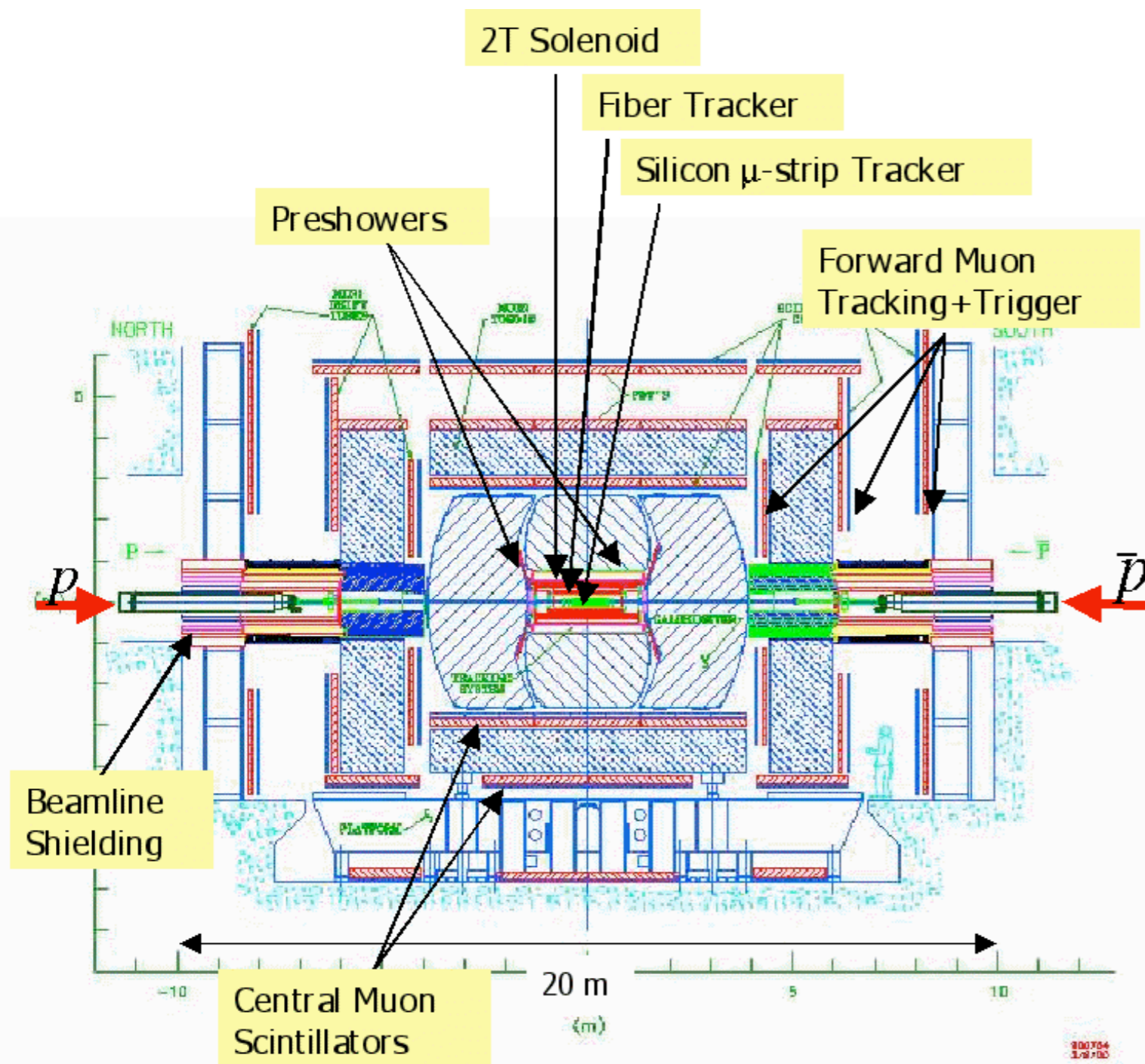
Fermilab 00-635

Run I: 6p and 6anti-p bunches with 3500ns bunch crossing spacing at $\sqrt{s}=1.8\text{TeV}$.
Run II: 36p and 36 anti-p bunches with 396ns spacing at $\sqrt{s}=1.96\text{TeV}$. Instantaneous luminosity exceeds $4 \times 10^{32} \text{ cm}^{-2}\text{s}^{-1}$.

The CDF detector



The D0 detector



18 countries
79 universities & institutes
399 people

Run I Higgs Results

Table 1: Table summarising the results for the SM Higgs searches showing for each channel the corresponding luminosity, branching ratio \times acceptance, expected background and observed events.

Channel	Experi- ment	$\int \mathcal{L}$ (pb ⁻¹)	BR \times Accept.(%) for M_H (GeV/c ²)			Expected background	Observed events	
b-tags			90	110	130			
$\ell\nu b\bar{b}$	1	CDF ³	106	.55 \pm .14	.74 \pm .18	.89 \pm .22	30 \pm 5	36
$\ell\nu b\bar{b}$	2	CDF ³	106	.23 \pm .06	.29 \pm .07	.34 \pm .09	3.0 \pm 0.6	6
$\ell\nu b\bar{b}$	1	DØ ⁴	106	.30 \pm .02	.36 \pm .02	.44 \pm .03	25.5 \pm 3.3	27
$\nu\nu b\bar{b}$	1	CDF	88	.59 \pm .12	.69 \pm .14	.86 \pm .17	39.2 \pm 4.4	40
$\nu\nu b\bar{b}$	2	CDF	88	.37 \pm .08	.44 \pm .11	.53 \pm .11	3.9 \pm 0.6	4
$\ell\ell b\bar{b}$	1	CDF	106	.14 \pm .03	.20 \pm .04	.19 \pm .04	3.2 \pm 0.7	5
$q\bar{q} b\bar{b}$	2	CDF ⁵	91	1.3 \pm .4	2.2 \pm .6	3.1 \pm .8	594 \pm 30	589

$WH \rightarrow \ell\nu b\bar{b}$

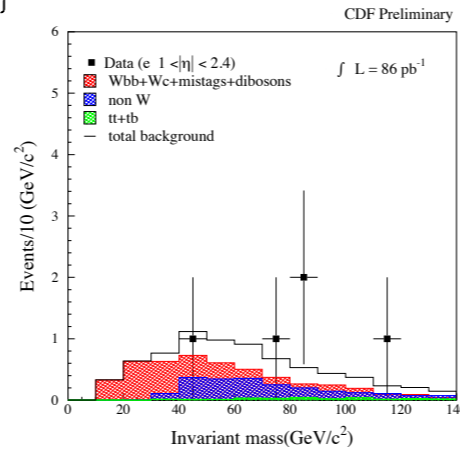
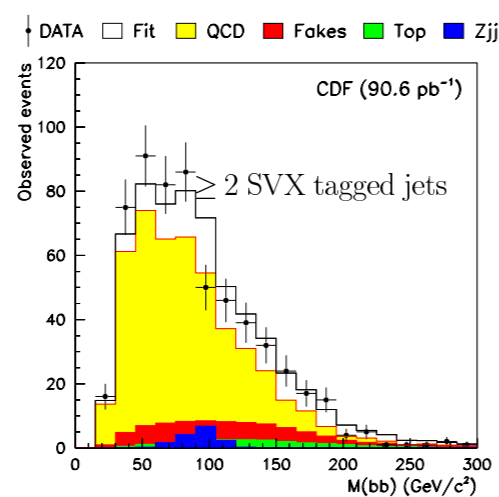
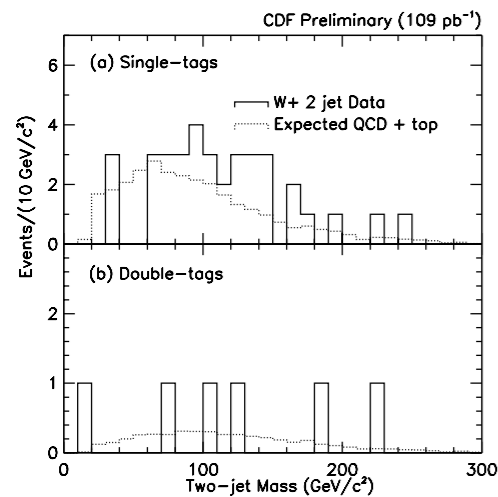
Expect : 30 \pm 5 st, 6.0 \pm 0.6 dt

Observe : 36 st, 6 dt

$VH \rightarrow q\bar{q} b\bar{b}$

Expect : 600 events

Observe : 589 events



$ZH \rightarrow \ell^+\ell^- b\bar{b}$

Expect : 3.2 \pm 0.7 st

Observe : 5

$ZH \rightarrow \nu\nu b\bar{b}$

Expect : 39.2 \pm 4.4 st, 3.9 \pm 0.6 dt

Observe : 40 st, 4 dt

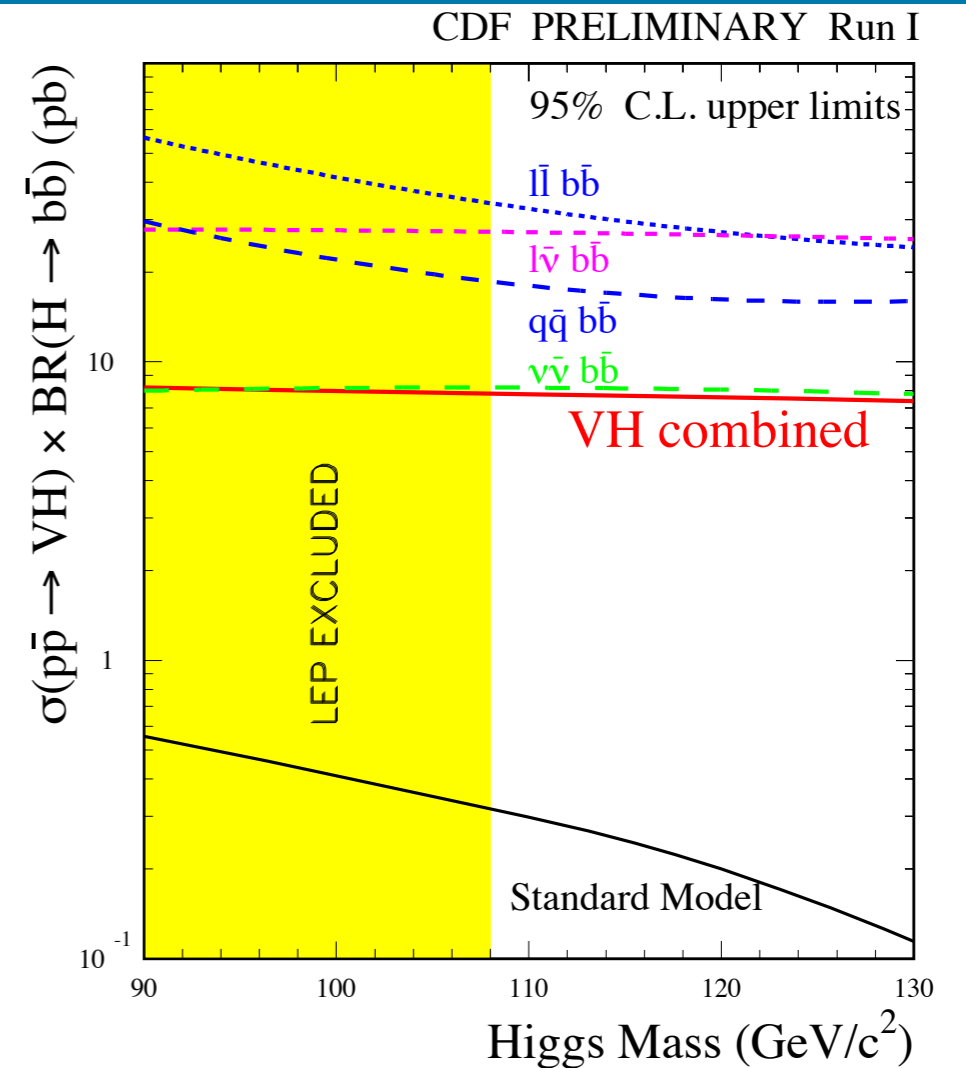
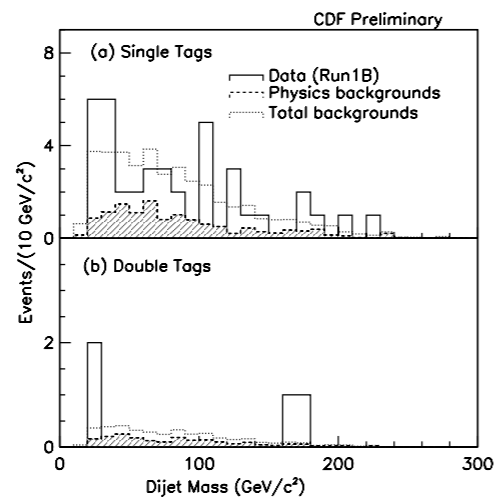
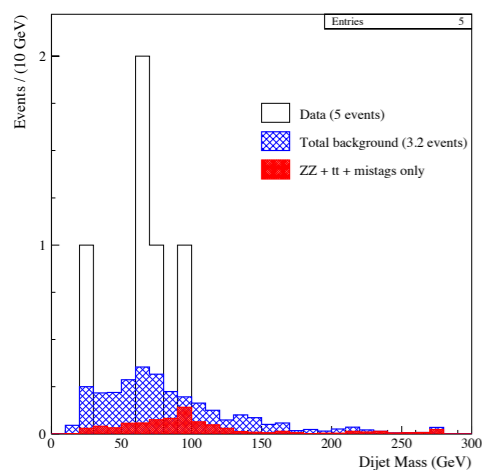


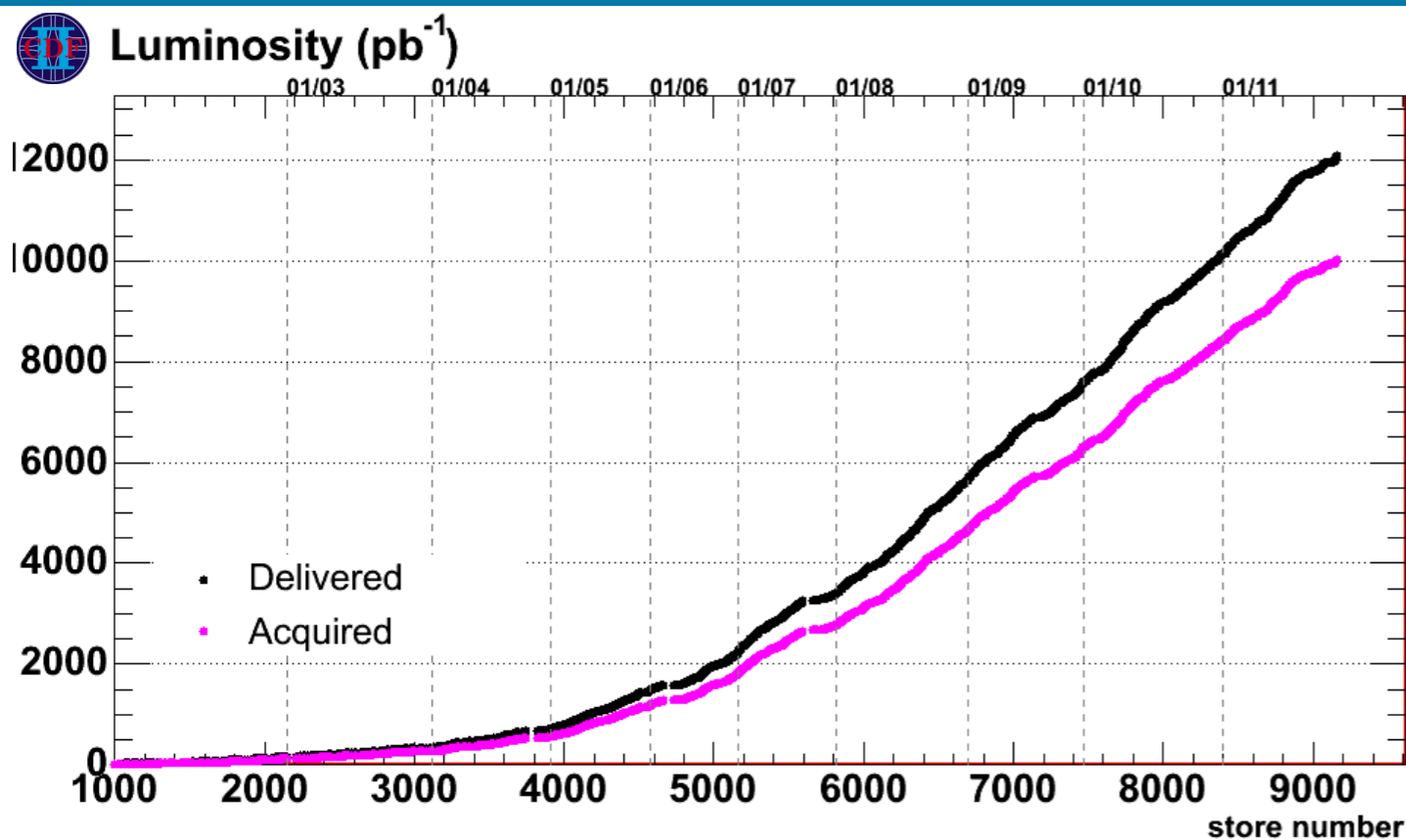
FIGURE 20. CDF Run 1 95% CL upper limits on the cross section times branching ratio for production of a Standard Model Higgs boson in association with a W or Z, with Higgs decaying to $b\bar{b}$ [136]. The four dashed curves show the limits from the individual search channels, and the solid curve labeled “VH combined” shows the limit from combining all four channels. The expectation from Standard Model Higgs production is shown by the solid curve labeled “Standard Model.”
FERMILAB Conf-96/258-E

Results from a Search for a Neutral Scalar Produced in Association with a W Boson in $p\bar{p}$ Collisions at $\sqrt{s} = 1.8$ TeV.

The DØ Collaboration¹
(July 1996)

This paper presents a search for production of a hypothetical heavy particle X in association with a W boson. For the search presented here, the kinematics and acceptances are modelled under the assumption that the X particle has the spin and decay properties of the standard model Higgs boson with the modification that only $X \rightarrow b\bar{b}$ decays are allowed. The W is required to decay via either the electron or muon mode. The complete DØ 1992-1995 data set is used. This sample has an integrated luminosity of 100 pb^{-1} and was taken at a center-of-mass energy of 1.8 TeV. Limits are set on the number of associated production events and the production cross section.

Run II: Integrated Luminosity

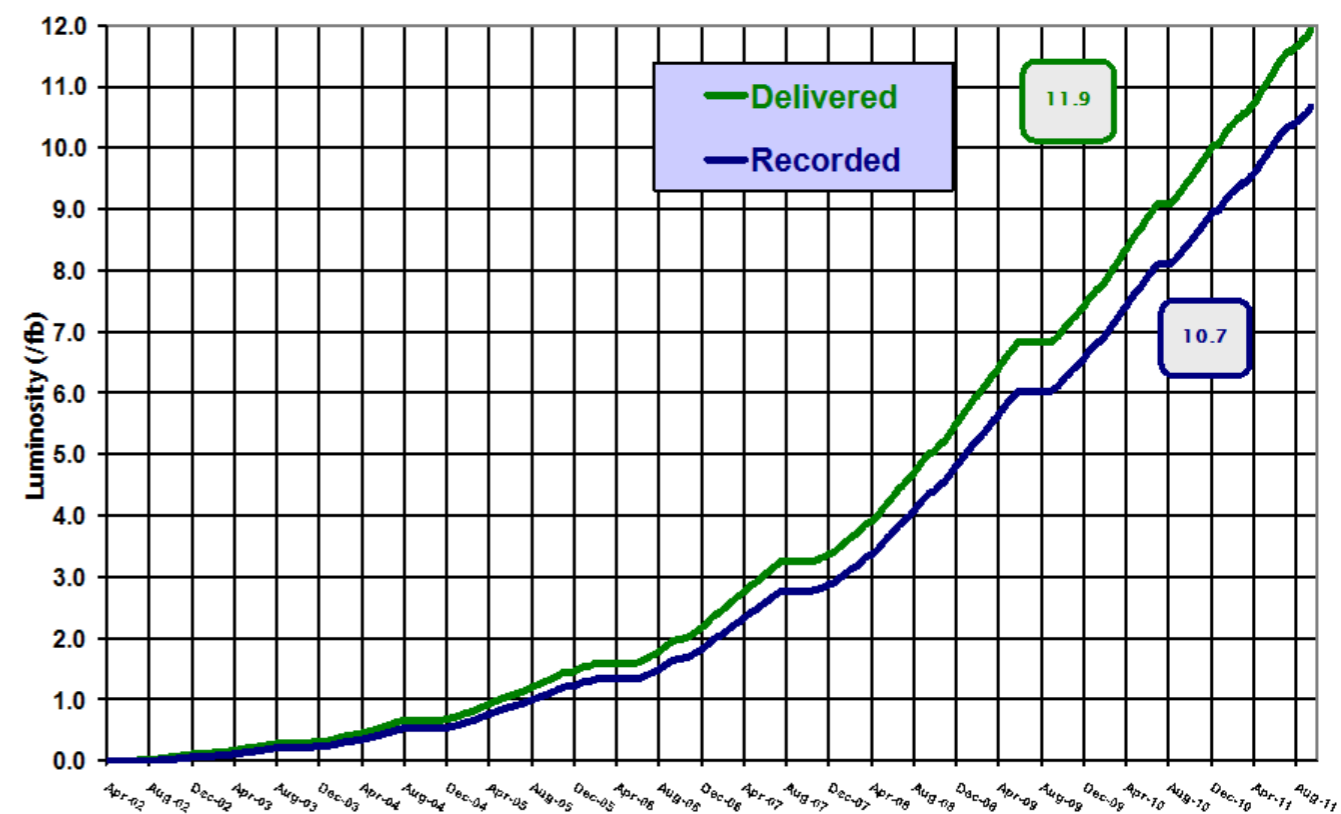


TeVatron delivered $\sim 12\text{fb}^{-1}$ to each experiment
 $\sim 10\text{fb}^{-1}$ recorded per experiment



Run II Integrated Luminosity

19 April 2002 - 30 September 2011



TeVatron Higgs Sensitivity Study: Initial Projection

FERMILAB-Conf-00/279-T
SCIPP 00/37
hep-ph/0010338
October 31, 2000

Report of the Tevatron Higgs Working Group

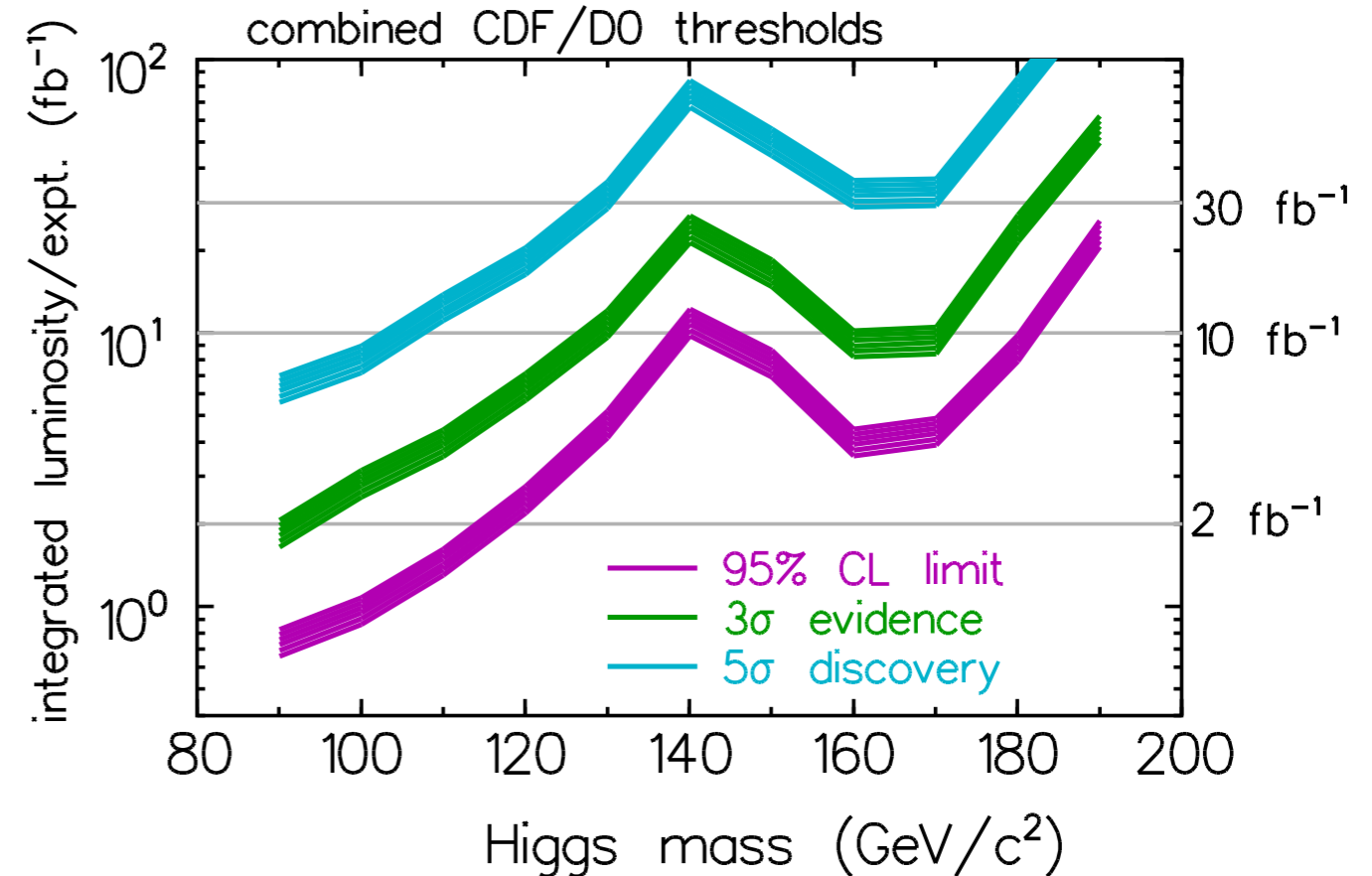


FIGURE 103. The integrated luminosity required per experiment, to either exclude a SM Higgs boson at 95% CL or discover it at the 3σ or 5σ level, as a function of the Higgs mass. These results are based on the combined statistical power of both experiments. The curves shown are obtained by combining the $\ell\nu b\bar{b}$, $\nu\bar{\nu} b\bar{b}$ and $\ell^+\ell^- b\bar{b}$ channels using the neural network selection in the low-mass Higgs region ($90 \text{ GeV} \lesssim m_{h_{\text{SM}}} \lesssim 130 \text{ GeV}$), and the $\ell^\pm\ell^\pm jj$ and $\ell^+\ell^-\nu\bar{\nu}$ channels in the high-mass Higgs region ($130 \text{ GeV} \lesssim m_{h_{\text{SM}}} \lesssim 200 \text{ GeV}$). The lower edge of the bands is the calculated threshold; the bands extend upward from these nominal thresholds by 30% as an indication of the uncertainties in b -tagging efficiency, background rate, mass resolution, and other effects.

Given the above discussion, the basic conclusions arrived at below are not unreasonably aggressive. Break-throughs in technique are always possible, and have indeed been the norm in the past. For example both the Higgs search in LEP1 and the top quark search in Run 1 at the Tevatron exceeded the expectations of studies prior to machine turn-on. The studies presented here should be taken as cautiously optimistic: Using full mass spectrum fits, applying neural network techniques, improving the trigger efficiencies, adding other search mode, and improving the mass resolution and tagging efficiency beyond that projected here may all serve to dramatically improve the discovery potential for the Higgs at the Tevatron.

TeVatron Higgs Sensitivity Study: Update

FERMILAB-PUB-03/320-E
October 17, 2003

Results of the Tevatron Higgs Sensitivity Study

CDF and DØ Collaborations

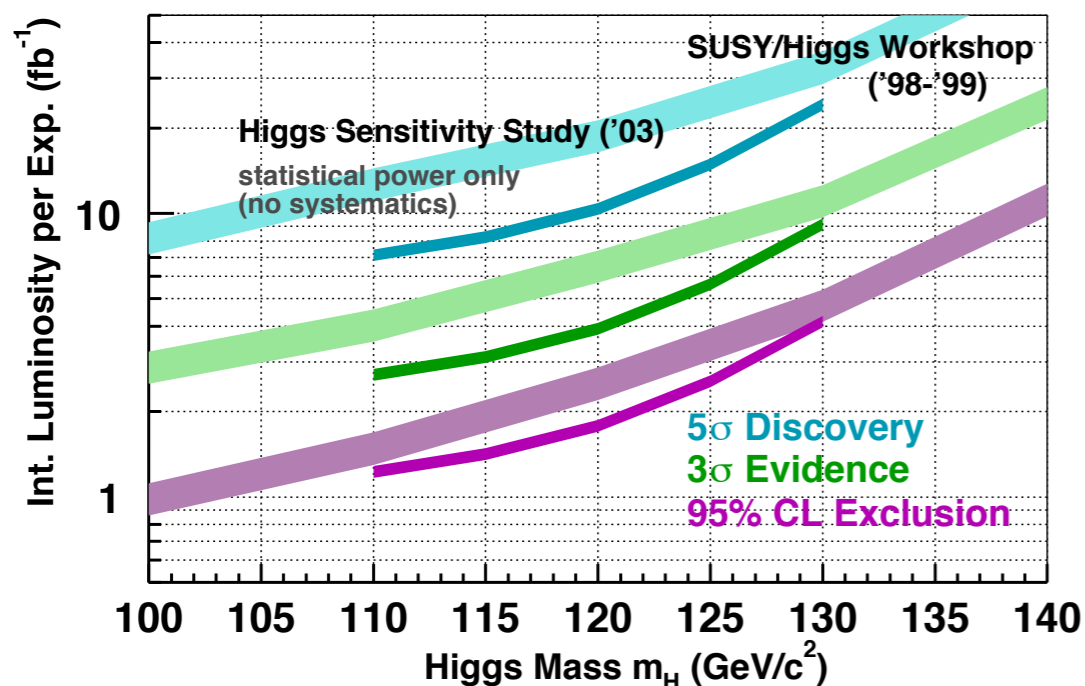


Figure 24: Integrated luminosities per experiment corresponding to the median expectations for 95% confidence level exclusion, 3σ evidence and 5σ discovery for $m_H = 110 - 130 \text{ GeV}/c^2$. The narrow curves are the updated analysis from this study (2003) and the thicker curves are the results from the previous SHWG Study (1999).

9 Conclusions and Summary

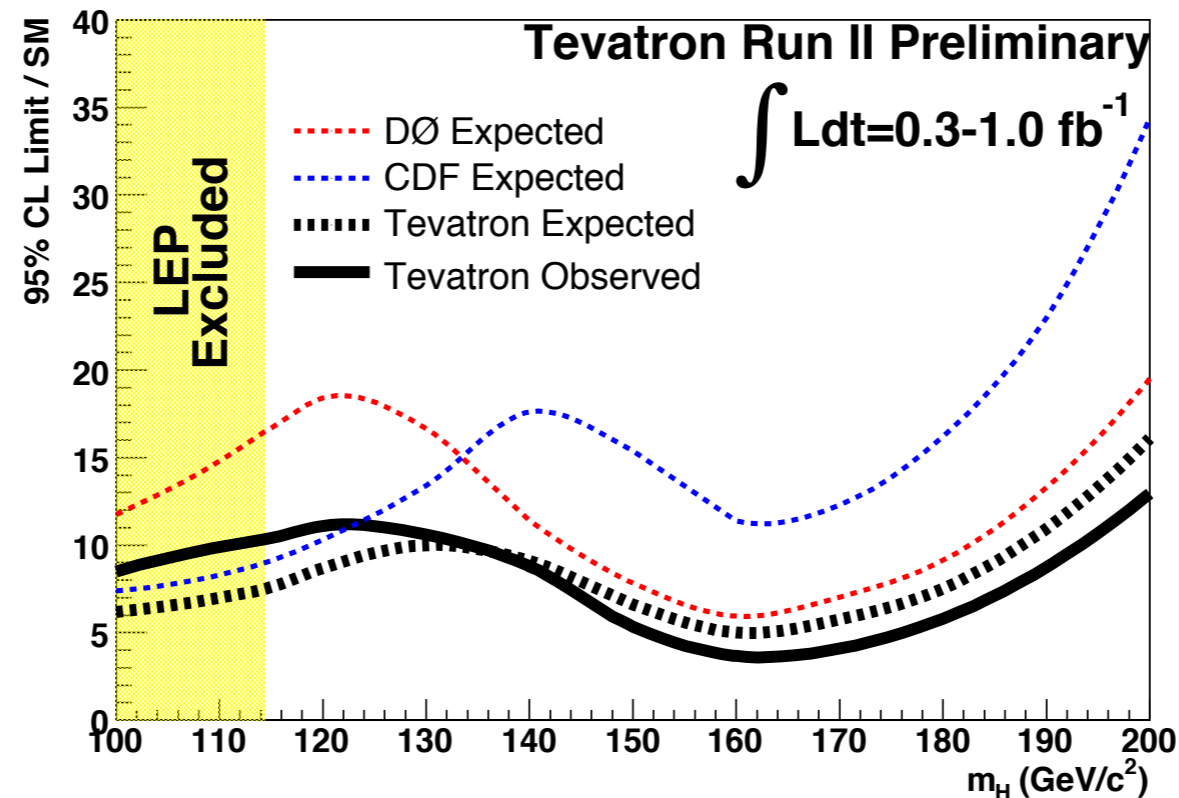
The results of this study show a reduction in the amount of integrated luminosity required to search for the Higgs boson at the Tevatron collider relative to the previous SUSY-Higgs Working Group study. The following improvements were verified with detailed analyses:

- The efficiencies of triggers, lepton identification, as well as other selection criteria, are based on Run II data. The b -tagging efficiencies, one of the most crucial performance parameters in the search for the Higgs boson, are based on GEANT simulations of the Run IIA and Run IIB detectors and projected luminosities and have been tied to Run IIA data.
- The study of the dijet mass resolution in the $\ell\nu b\bar{b}$ analysis indicates that a mass resolution of 10% may be experimentally achievable.
- The accuracy of the QCD background estimate in the $\nu\nu b\bar{b}$ analysis was substantially improved by applying the event selection to the Run II data and using Monte Carlo generators to estimate the b -quark content.
- An advanced neural network analysis reduces dramatically the amount of $t\bar{t}$ background while keeping a large fraction of the signal.
- The use of the shapes of the signal and background distributions gives an enhancement in the search sensitivity of approximately 20% in equivalent integrated luminosity.

The WH and ZH search modes were combined to estimate the full sensitivity of a DØ and CDF data analysis with $1-10 \text{ fb}^{-1}$ in the mass range $110-130 \text{ GeV}/c^2$. These results are summarized in Figure 24 and Table 21. A critical feature of these predictions is the ability to control systematic errors, especially on the dijet mass shape, for the signal and the backgrounds. Methods for controlling one of the primary classes of systematic uncertainty, namely, background rate uncertainties, are discussed. It is anticipated that further evaluation of the available data samples will give accurate estimates of several important background rates and detector efficiencies. In summary, the improvements in the Higgs search sensitivities come from a better use of signal information and more optimized methods of analysis. Further developments of this type are foreseen in a full complement of analyses from the two experiments.

TeVatron 2006: First Combined Limits

- **Mid-2005: first fb^{-1}**
- **2006: first CDF+D0 limits:**



D0 **260 – 950 pb^{-1}**

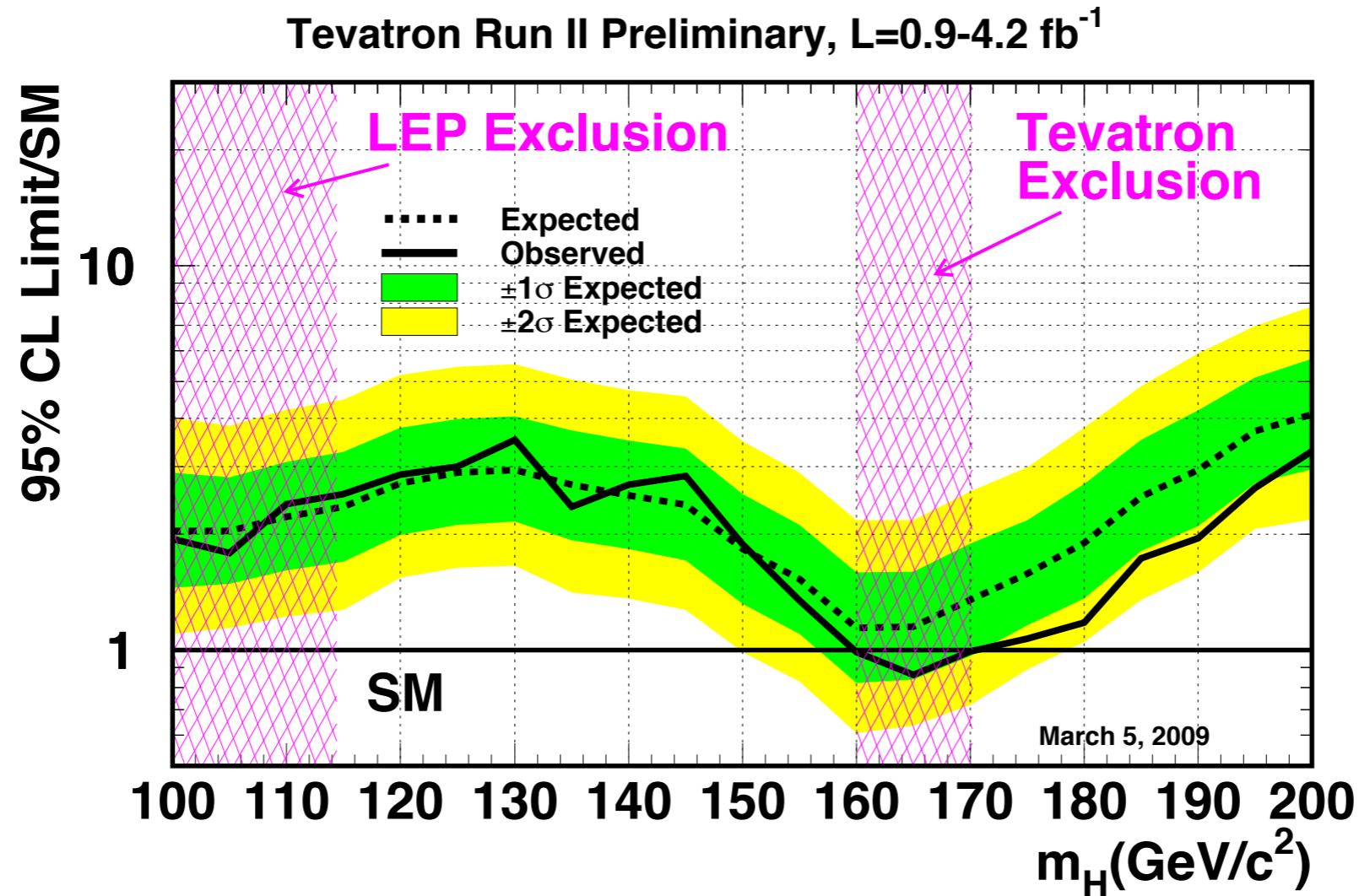
CDF **360 – 1000 pb^{-1}**

- **Limits: 10.4 (3.8) times SM**
@ $m_H = 115(160) \text{ GeV}$
- [CDF Note 8384, D0 note 5227](#)

TeVatron 2009: First exclusions

Winter 2009: First mass range excluded after LEP
(at 95%CL): $160 < m_H < 170 \text{ GeV}$

D0	0.9 – 4.2 fb ⁻¹
CDF	2.0 – 3.6 fb ⁻¹

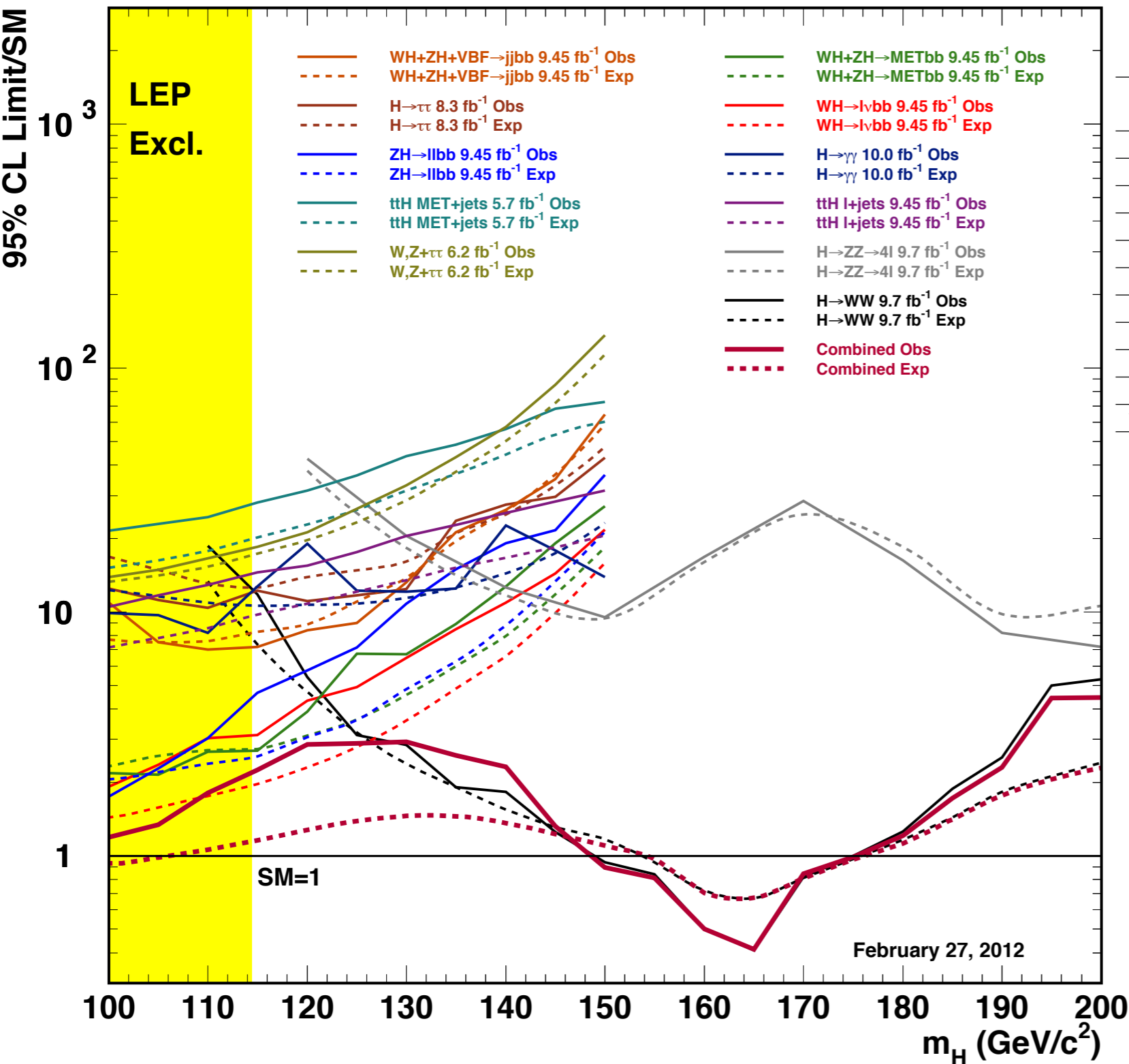


- Channels:
- **Production:** $q\bar{q} \rightarrow W/ZH$, $gg \rightarrow H$, $q\bar{q} \rightarrow q'\bar{q}'H$ (VBF)
 - **Decay:** $H \rightarrow b\bar{b}$, $H \rightarrow W^+W^-$, $H \rightarrow \tau^+\tau^-$, $H \rightarrow \gamma\gamma$

CDF Overview of Searches

CDF Note 10804

CDF Run II Preliminary, $L \leq 10.0 \text{ fb}^{-1}$



@ $m_H=125 \text{ GeV}$

Channel	Dataset [fb^{-1}]	Limit Expected σ/σ_{SM}	Limit Observed σ/σ_{SM}
$WH \rightarrow \ell\nu bb$	9.45	2.79	4.93
$H \rightarrow WW$	9.7	3.08	2.98
$VH \rightarrow \text{MET} + bb$	9.45	3.62	6.75
$ZH \rightarrow \ell\ell bb$	9.45	3.6	7.2
$H \rightarrow \gamma\gamma$	10.0	10.8	12.2
$VH \rightarrow qqbb + Hqq \rightarrow qqbb$	9.45	11.0	9.0
$ttH \rightarrow \ell + \text{jets}$	9.4	12.4	17.6
$H \rightarrow \tau\tau$	8.3	14.8	11.7
$V + \tau\tau$	6.2	23.3	26.5
$H \rightarrow ZZ \rightarrow 4\ell @130 \text{ GeV}$	9.7	18.3	20.5
$ttH \rightarrow \text{MET} + \text{jets}/\text{All jets}$	5.7	26.2	36.2



An Example Analysis: CDF WH(\rightarrow lvbb)

- Analyzed the 9.45 fb^{-1} of the full dataset recorded by CDF
- Triggers for high energy electrons, muons or large missing transverse energy
- Final State: high energy lepton candidates, large missing transverse energy, and 2 or 3 jets ≥ 1 b-tag
Jets $E_T > 20 \text{ GeV}$ $|\eta| < 2.0$

Main improvement comparing to the previous result comes from improved b-jet tagging algorithm.

Previously: combination of three b-jet taggers.

Now: Newly developed multivariate b-jet tagger, the **Higgs-Optimized b-Identification Tagger** (HOBIT)

Two HOBIT operational points: We denote them as Tight ($\epsilon_b = 0.72$) and Loose ($\epsilon_b = 0.98$) respectively.

5 orthogonal b-tagging categories are defined: **TT, TL, LL, T, and L**. [TT, and TL only for 3 jet events]

Events classified into dedicated lepton categories: **central tight leptons, forward electrons, loose muons and loose electron-like leptons**. Where the lepton-identification/trigger acceptance has been maximized (using relaxed lepton categories and combinations of triggers)

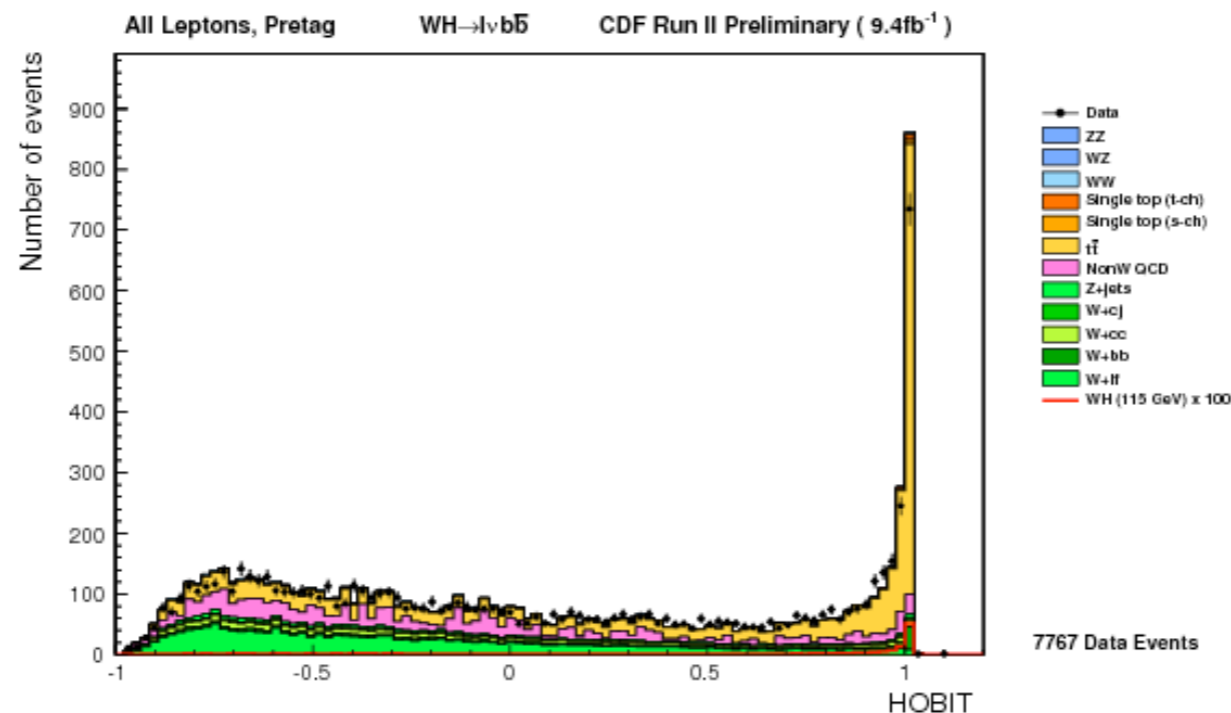
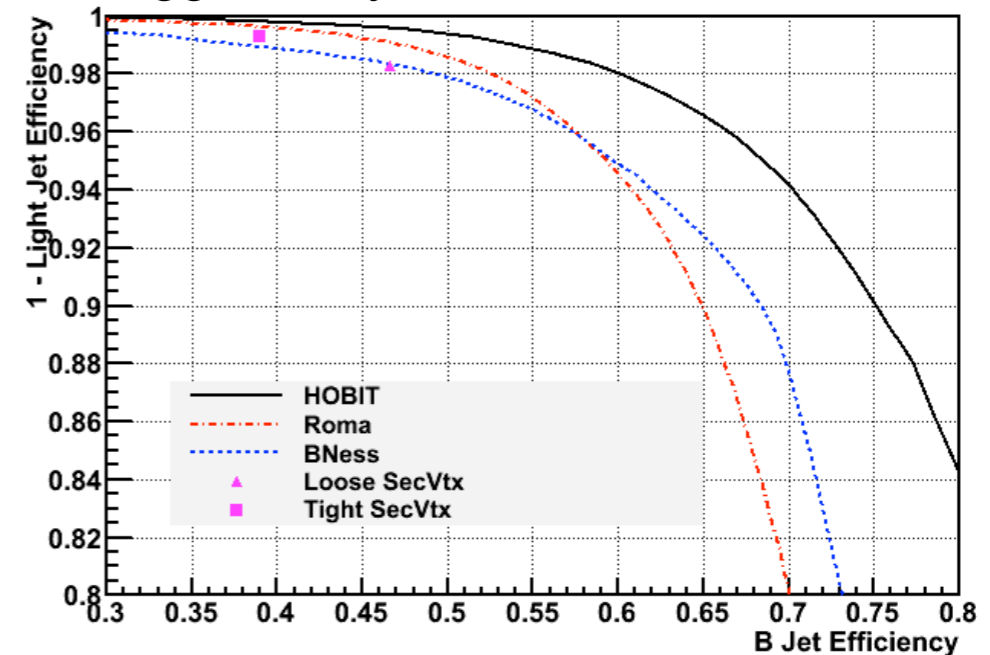
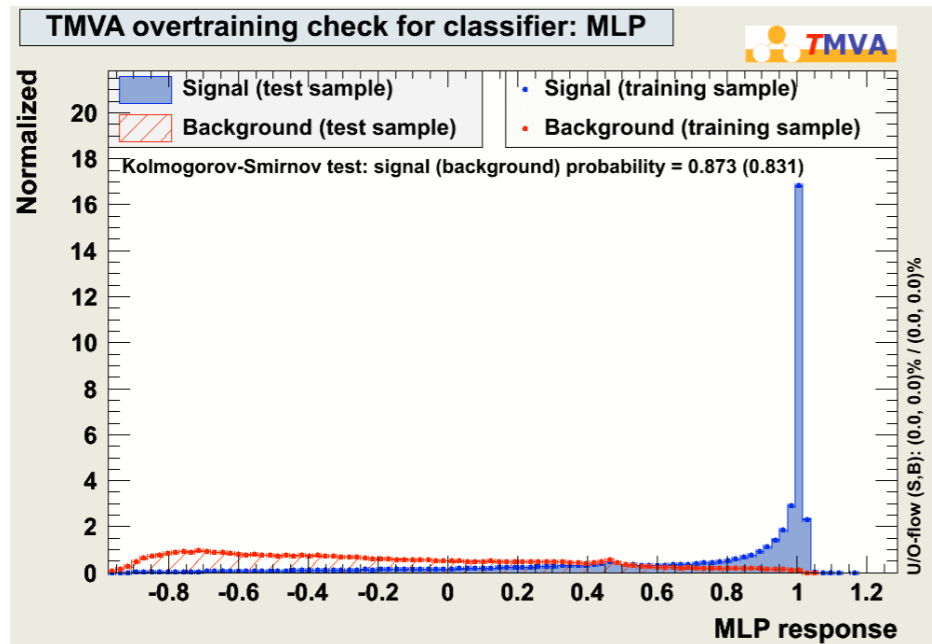
Offline, central electron or muon candidates are required offline to be isolated and have E_T (or p_T) $> 20 \text{ GeV}$ (GeV/c). Since the W +jets signature presents a large missing transverse energy, we require $\cancel{E}_T > 20 \text{ GeV}$ ($\cancel{E}_T > 10 \text{ GeV}$) for electrons (muons).

We increase the purity of the sample by applying cuts intended to remove multijet events due to QCD processes that include fake-lepton signatures. The QCD veto is based on the SVM multivariate technique, which uses different kinematical input variables [10]. Some of them are related to the W kinematics like the lepton p_T , \cancel{E}_T , or $\Delta\phi(\text{lepton}, \cancel{E}_T^{\text{uncorrected}})$. Some are related to the kinematics of the jets in the event like $\cancel{E}_T^{\text{uncorrected}}$ and the transverse energy of the second leading E_T jet. A variable denoted as \cancel{E}_T significance is also used. This variable is defined as the ratio of \cancel{E}_T to a weighted sum of factors correlated with mismeasurement, such as angles between the \cancel{E}_T and the jets and the amount of jet energy corrections.

For forward electrons and loose electron-like leptons the cut-based QCD veto used in previous iterations of this analysis is used [11]. This veto applies a linear cut on the \cancel{E}_T and the azimuthal angle (ϕ) between the \cancel{E}_T and each of the jets ($\cancel{E}_T > 45 - (30 \cdot |\Delta\phi|) \text{ GeV}$), requires a large transverse mass of the reconstructed W boson candidate ($M_T(W) > 20 \text{ GeV}$), and a large \cancel{E}_T significance.

An Example Analysis: CDF WH(\rightarrow lvbb)

The inputs to HOBIT are a combination of general jet properties, and inputs developed for SecVtx, Roma and BNess taggers. The training was performed using a sample of b-quark jets from Higgs to bb samples with a Higgs mass of 120 GeV as signal and light jets (udsg) from Alpgen W+jets samples. The light jets background sample was reweighted to have the same ET spectrum as the b-jets from Higgs decays.



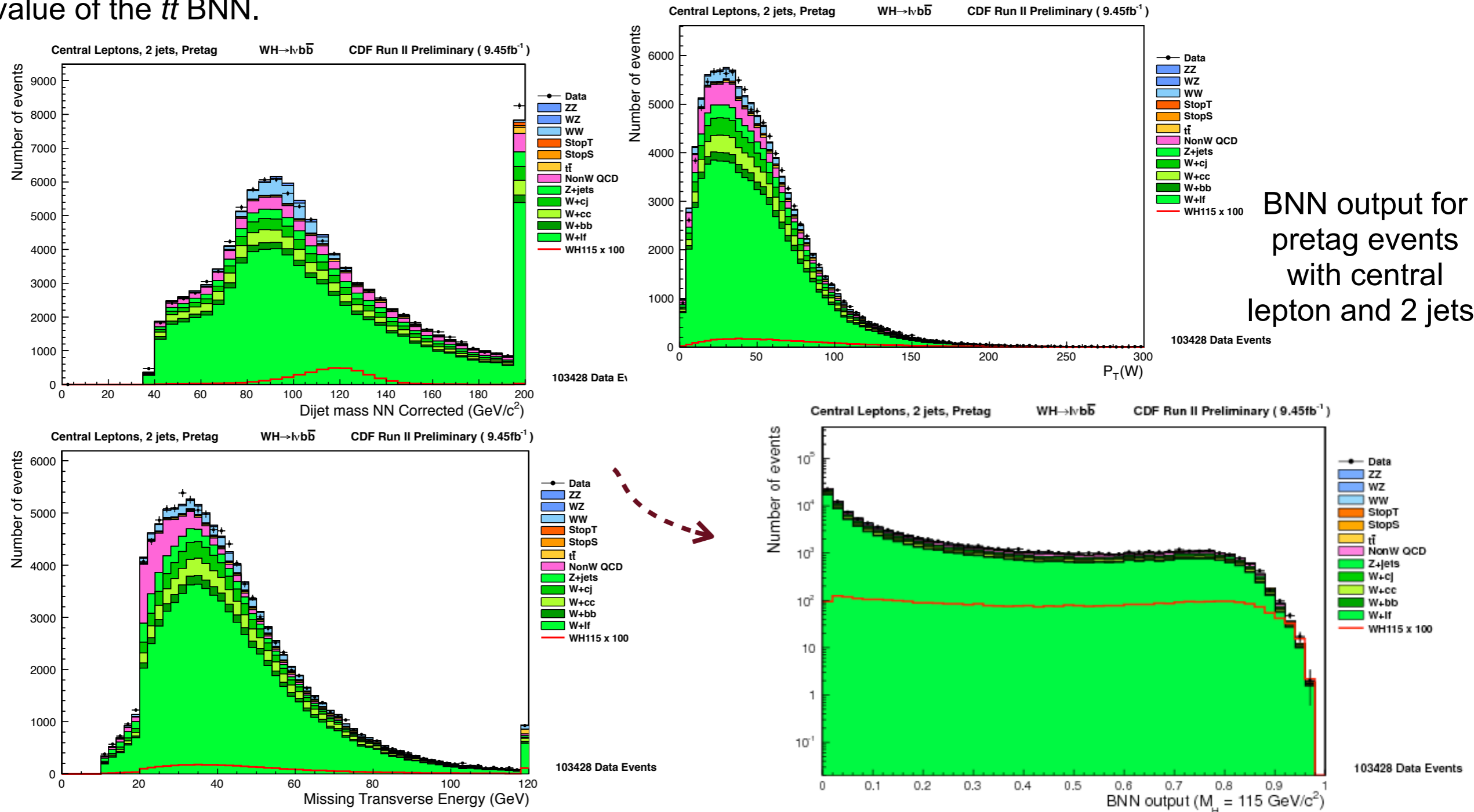
The HOBIT distribution for the highest Et jet in W+2/3/4/5 jet events, data vs. MC.

An Example Analysis: CDF WH(\rightarrow lvbb)

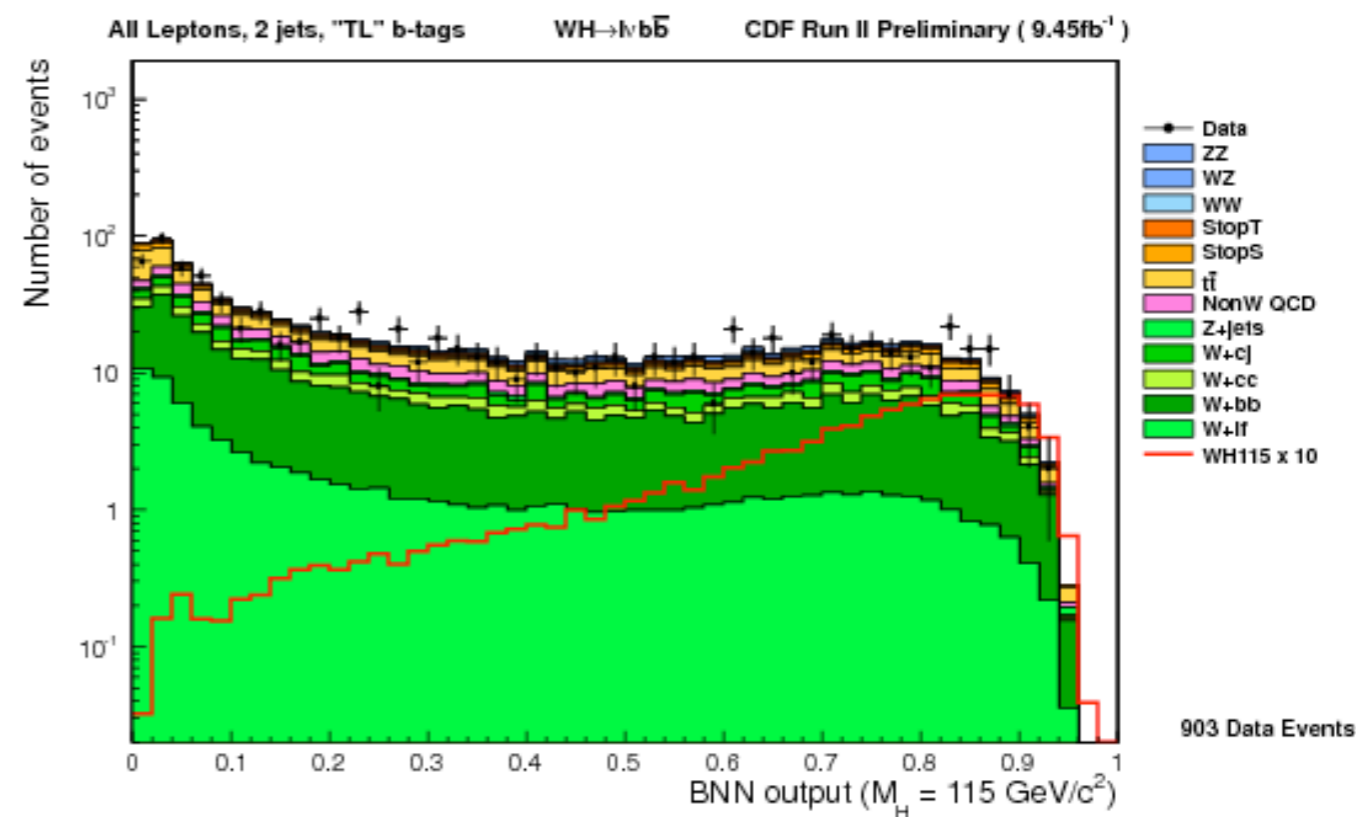
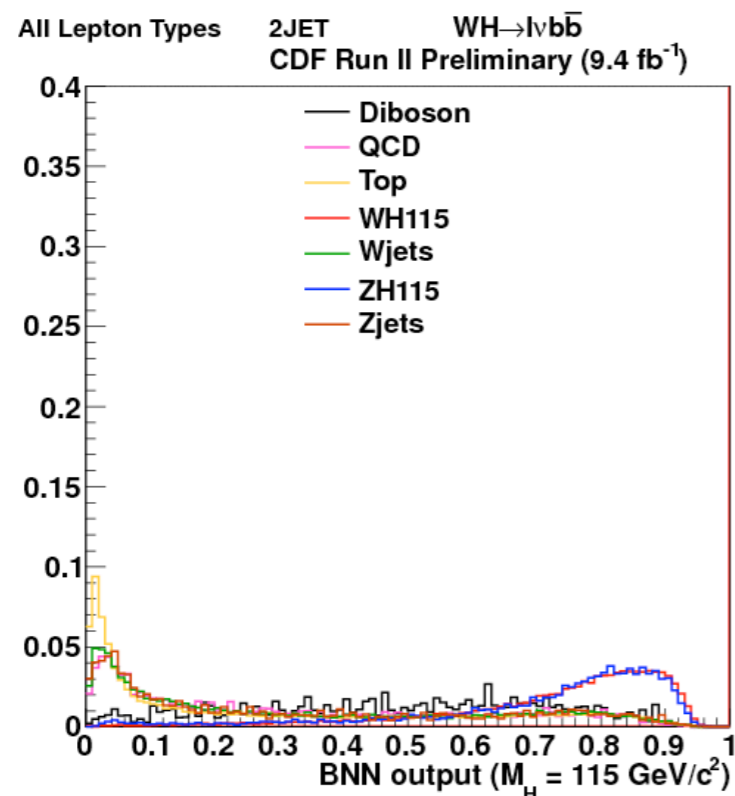
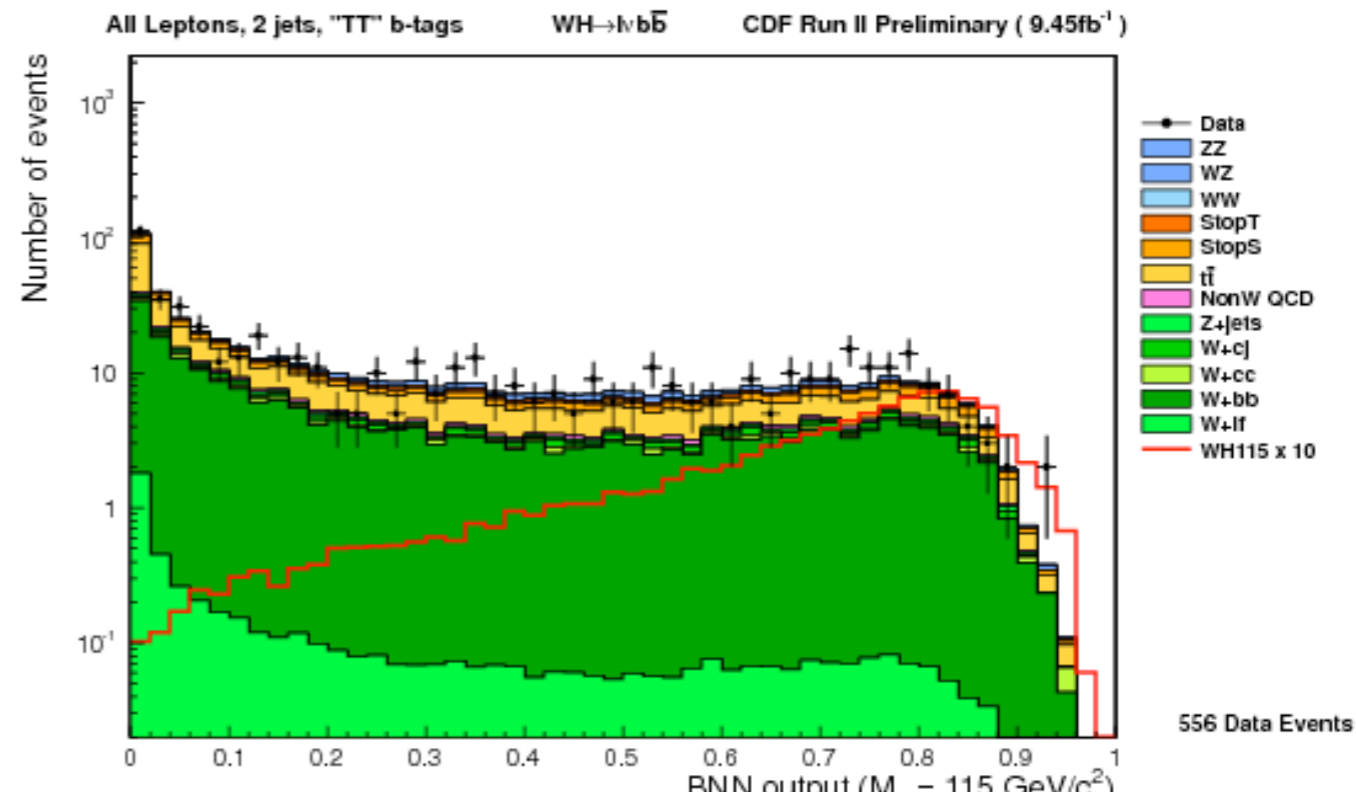
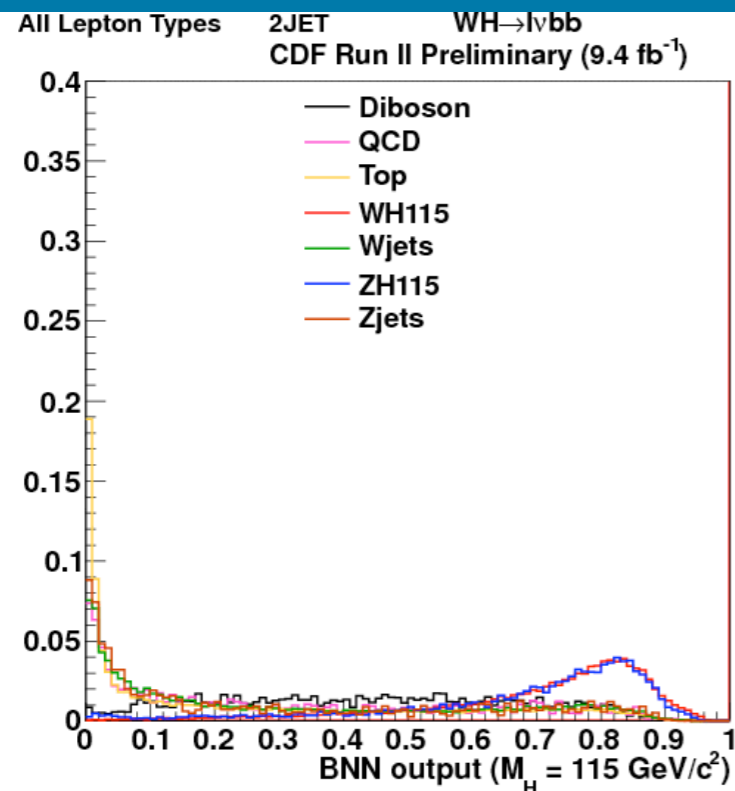
Number of Jets	2 jets					3 jets	
Tagging categories	TT	TL	T	LL	L	TT	TL
DiTop	177.49 \pm 22.17	211.19 \pm 19.8	544.5 \pm 52.06	63.04 \pm 6.93	327.74 \pm 33.71	495.7 \pm 61.59	581.77 \pm 54.47
S _{Top} S	59.1 \pm 7.06	66.39 \pm 5.85	118.38 \pm 10.68	19.35 \pm 2.19	69.4 \pm 7.13	19.34 \pm 2.33	22.66 \pm 2.01
S _{Top} T	17.4 \pm 2.48	32.45 \pm 3.98	228.45 \pm 25.63	12.21 \pm 1.32	134.83 \pm 15.56	22.13 \pm 3.03	29.87 \pm 3.32
WW	1.9 \pm 0.48	15.54 \pm 3.13	217.47 \pm 27.09	29.26 \pm 4.5	719.24 \pm 70.55	1.8 \pm 0.35	8.04 \pm 1.43
WZ	21.86 \pm 2.63	25.97 \pm 2.28	63.3 \pm 6.23	11.8 \pm 1	115.13 \pm 10.59	4.19 \pm 0.51	6 \pm 0.57
ZZ	2.6 \pm 0.3	2.73 \pm 0.24	7.87 \pm 0.77	1.08 \pm 0.09	11.98 \pm 1.08	0.96 \pm 0.11	1.22 \pm 0.11
Zjets	11.94 \pm 1.29	23.24 \pm 2.47	184.32 \pm 19.71	30.93 \pm 3.46	815.82 \pm 85.61	7.03 \pm 0.75	15.4 \pm 1.62
Wbb	284.99 \pm 116.78	382.43 \pm 155.86	1372.45 \pm 559.67	129.59 \pm 52.89	948.67 \pm 387.04	107.98 \pm 45.01	162.42 \pm 67.48
Wcc	22.54 \pm 9.39	141.43 \pm 58.32	1379.5 \pm 564.72	196.66 \pm 80.63	3332.54 \pm 1360.1	12.59 \pm 5.31	71.59 \pm 30.04
Wlf	5.17 \pm 1.54	73.93 \pm 16.53	1179.09 \pm 191.85	293.49 \pm 47.08	9732.87 \pm 1094.5	3.21 \pm 1.1	41.46 \pm 10.51
QCD	12.35 \pm 7.94	101.82 \pm 41.71	680.92 \pm 272.42	125.62 \pm 50.72	2031.95 \pm 812.95	5.79 \pm 5.17	68.53 \pm 28.41
Bkg	617.34 \pm 172.05	1077.12 \pm 309.74	5976.25 \pm 1730.5	913.03 \pm 250.76	18240.17 \pm 3877.7	680.72 \pm 125.24	1008.96 \pm 200.09
Obs	556	907	5737	865	18606	643	850
WH115	9.57 \pm 0.98	9.98 \pm 0.62	16.29 \pm 1.04	2.7 \pm 0.27	9.07 \pm 0.75	2.2 \pm 0.22	2.41 \pm 0.14

An Example Analysis: CDF WH(\rightarrow lvbb)

To take advantage of the kinematic differences between WH and SM background the final discriminant is constructed by means of Bayesian Neural Network (BNN). One for each b-tagging category (2 jets: **Double Tag Tight**, **Double Tag Loose**, and **Single Tag**, 3 jets: **Double Tag Tight**, and **Double Tag Loose**). For 3jets the BNN is trained against ttbar, a cut on this variable is applied to subsequently to train an additional BNN against the $W+bb$ background. The final discriminant separates the events in 2 regions according to the output value of the tt BNN.

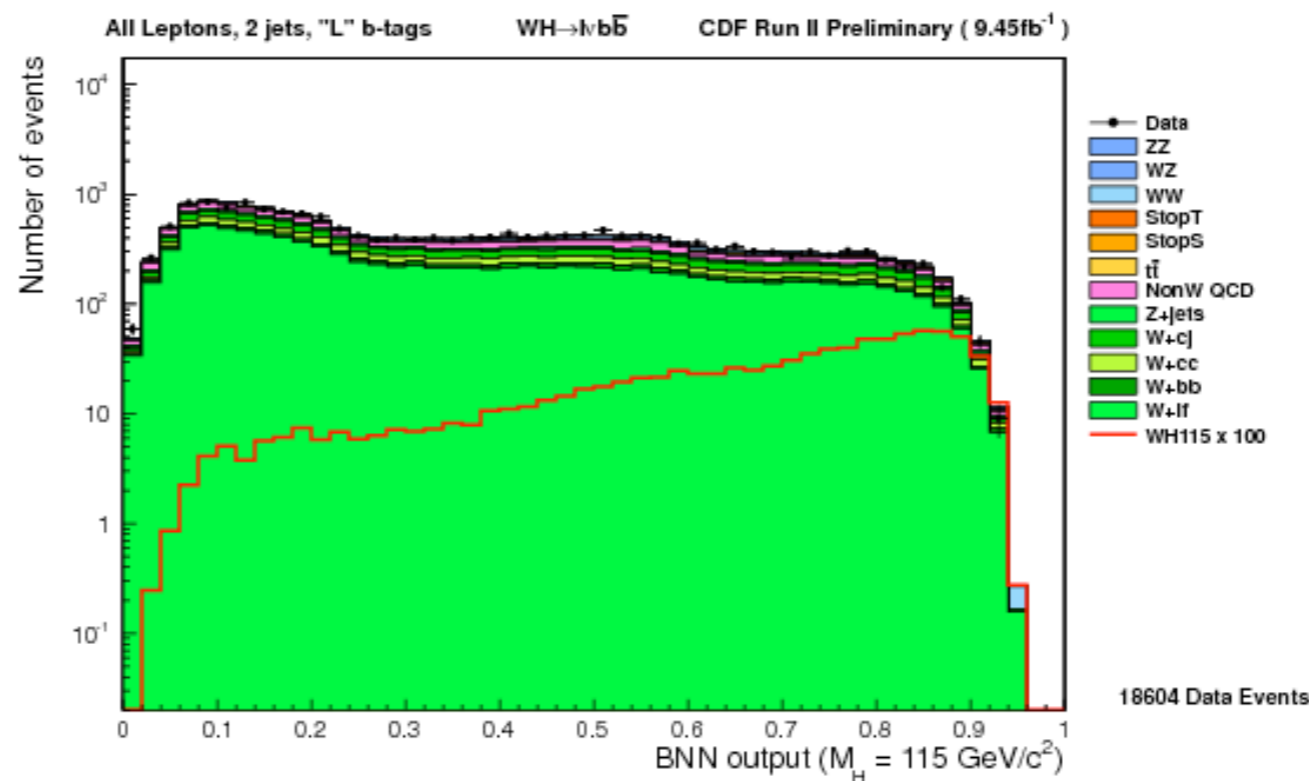
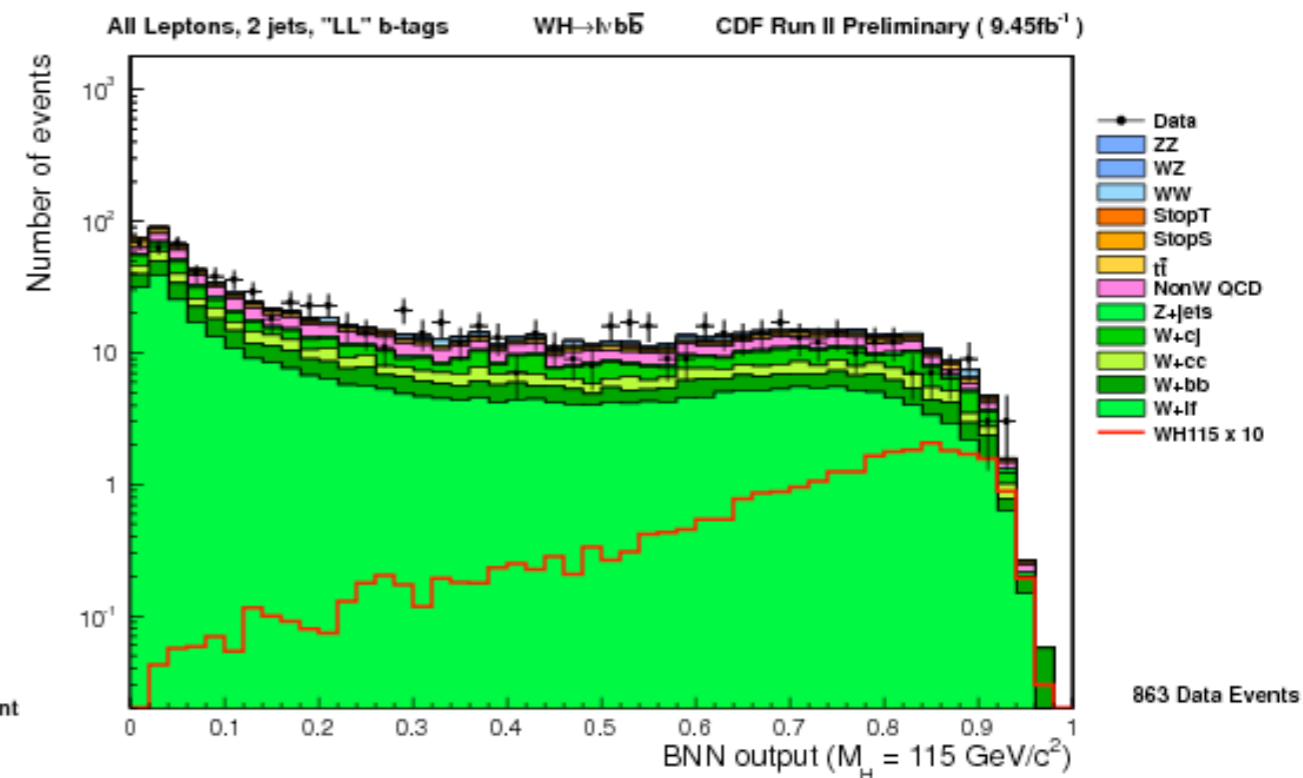
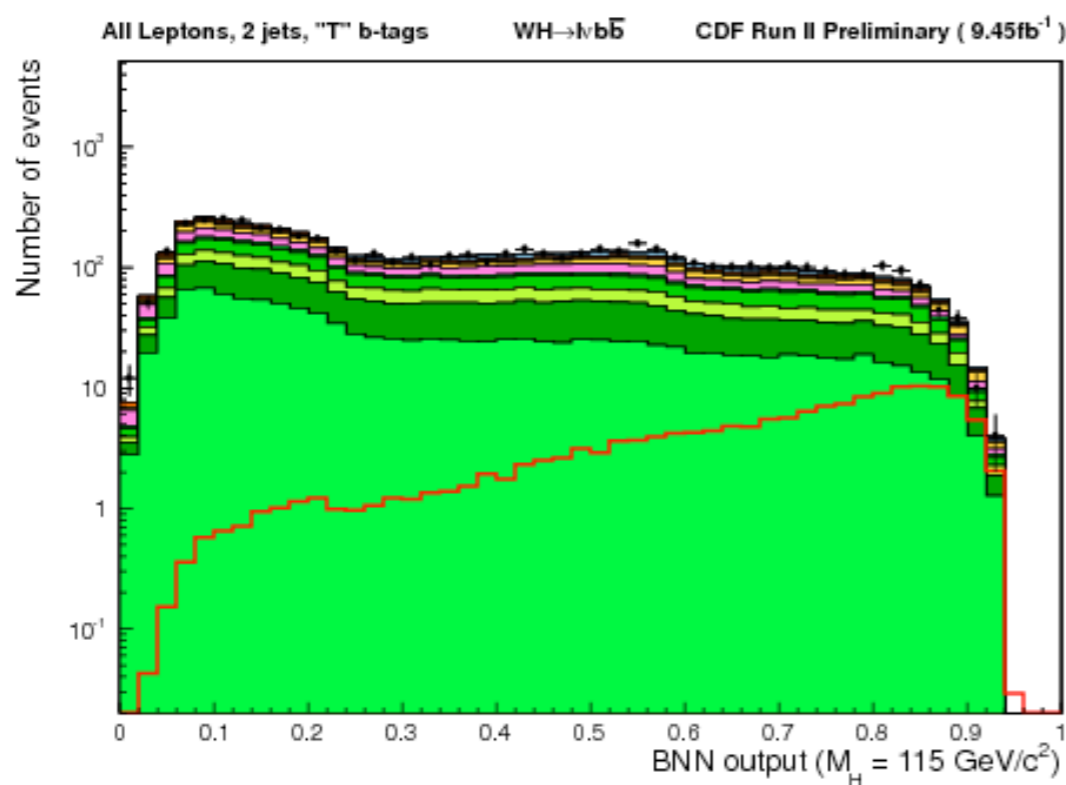


An Example Analysis: CDF WH(\rightarrow lvbb)

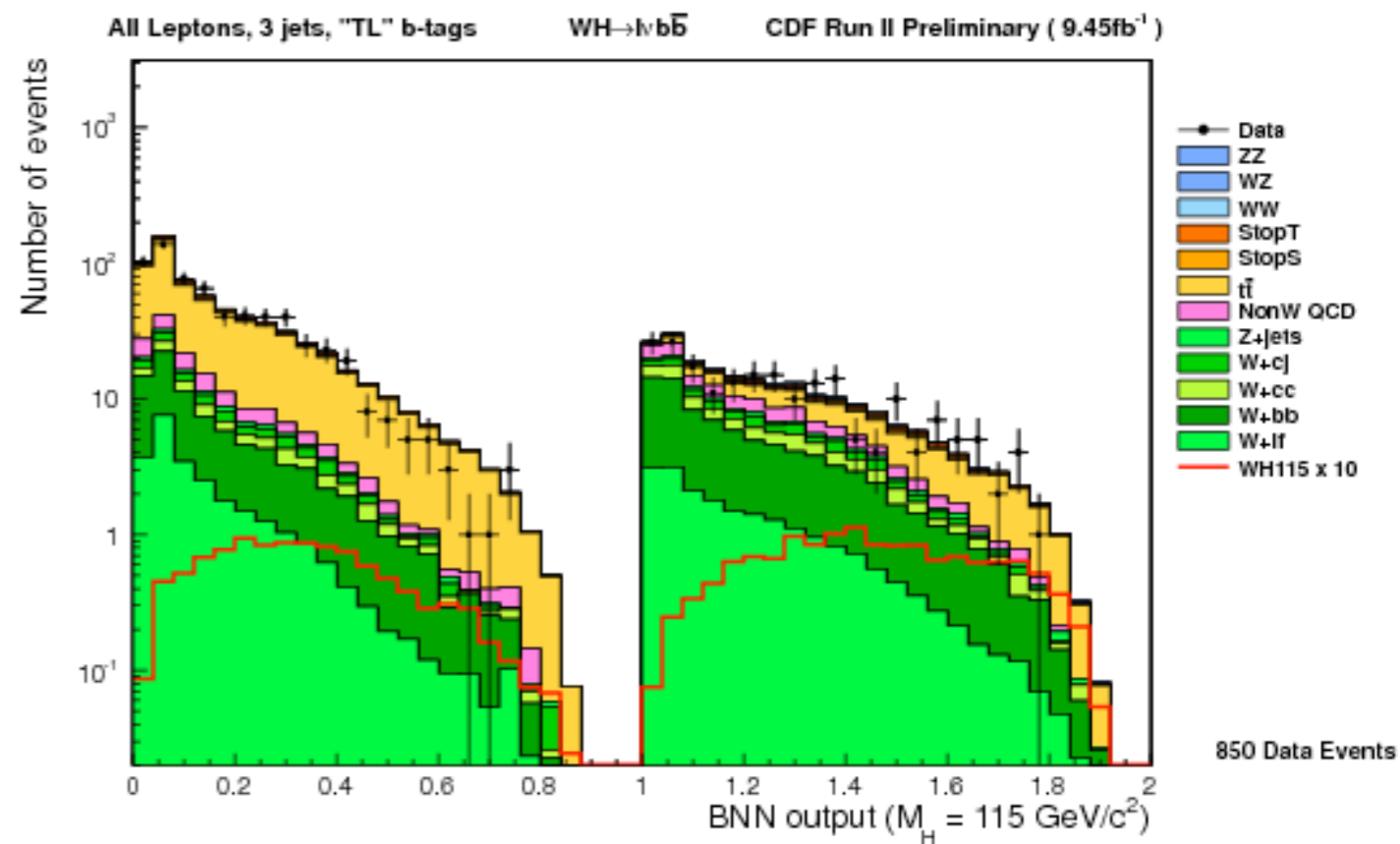
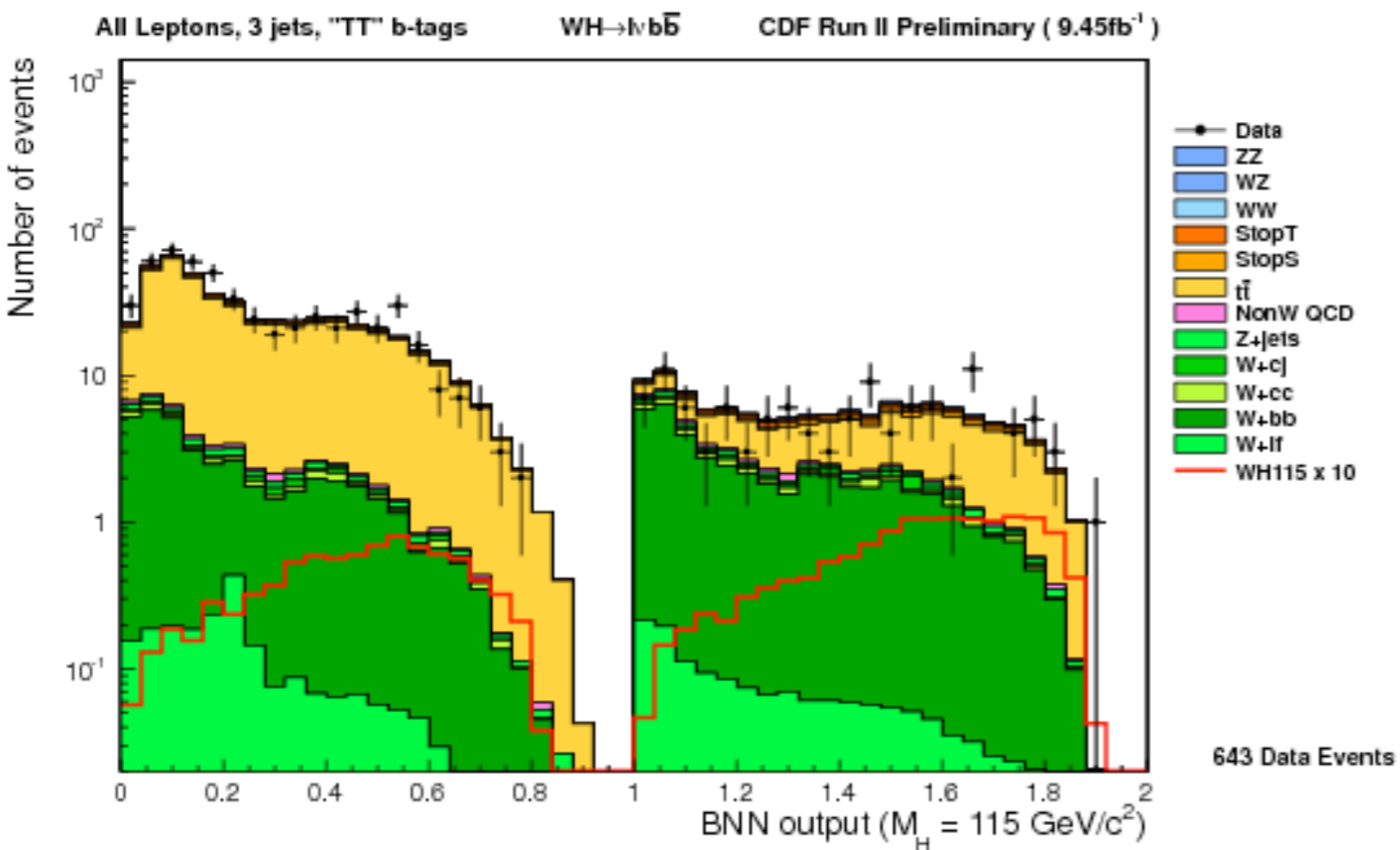


~75% of the analysis sensitivity comes from these two categories

An Example Analysis: CDF WH(\rightarrow lvbb)



An Example Analysis: CDF WH(\rightarrow lvbb)



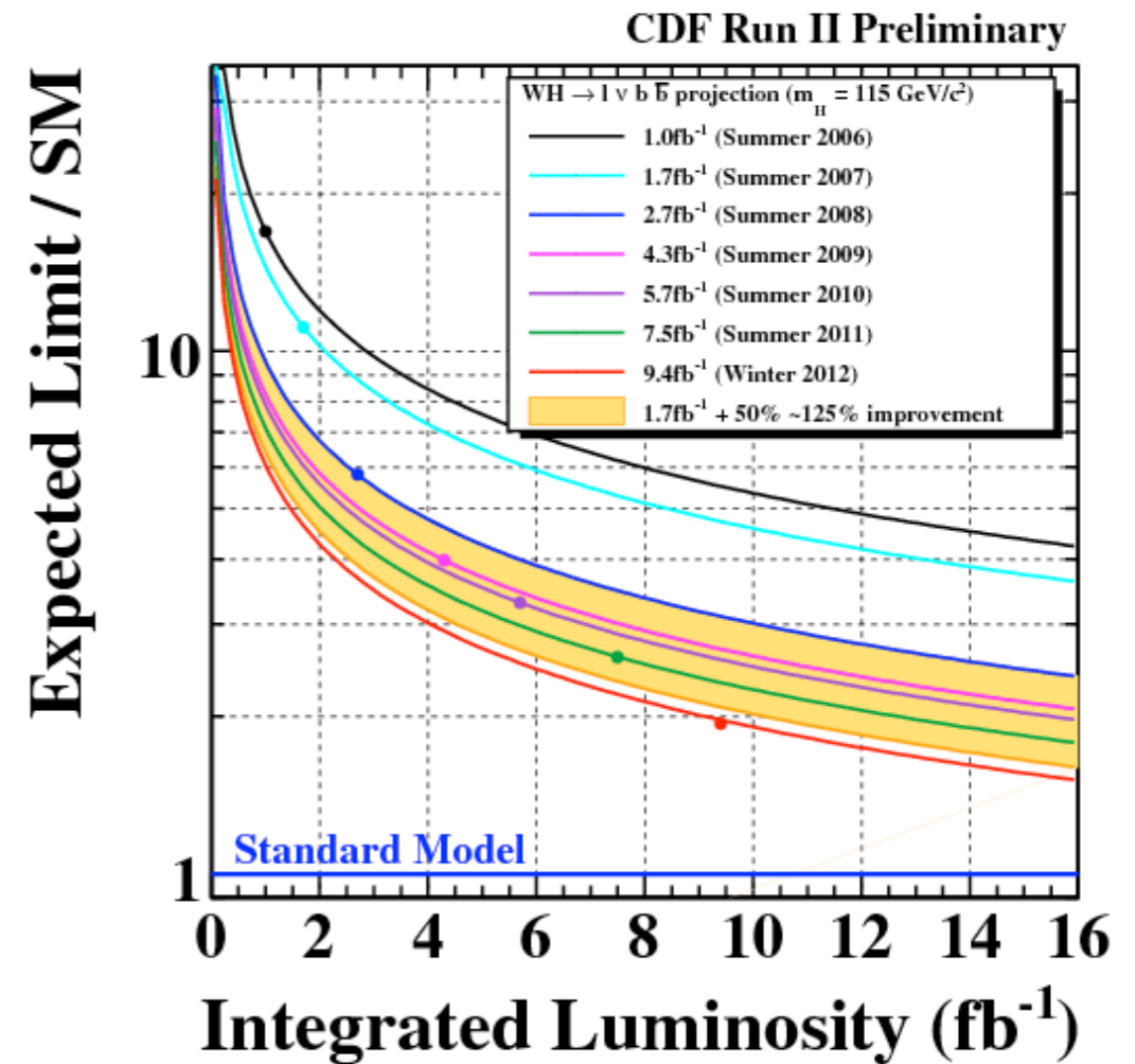
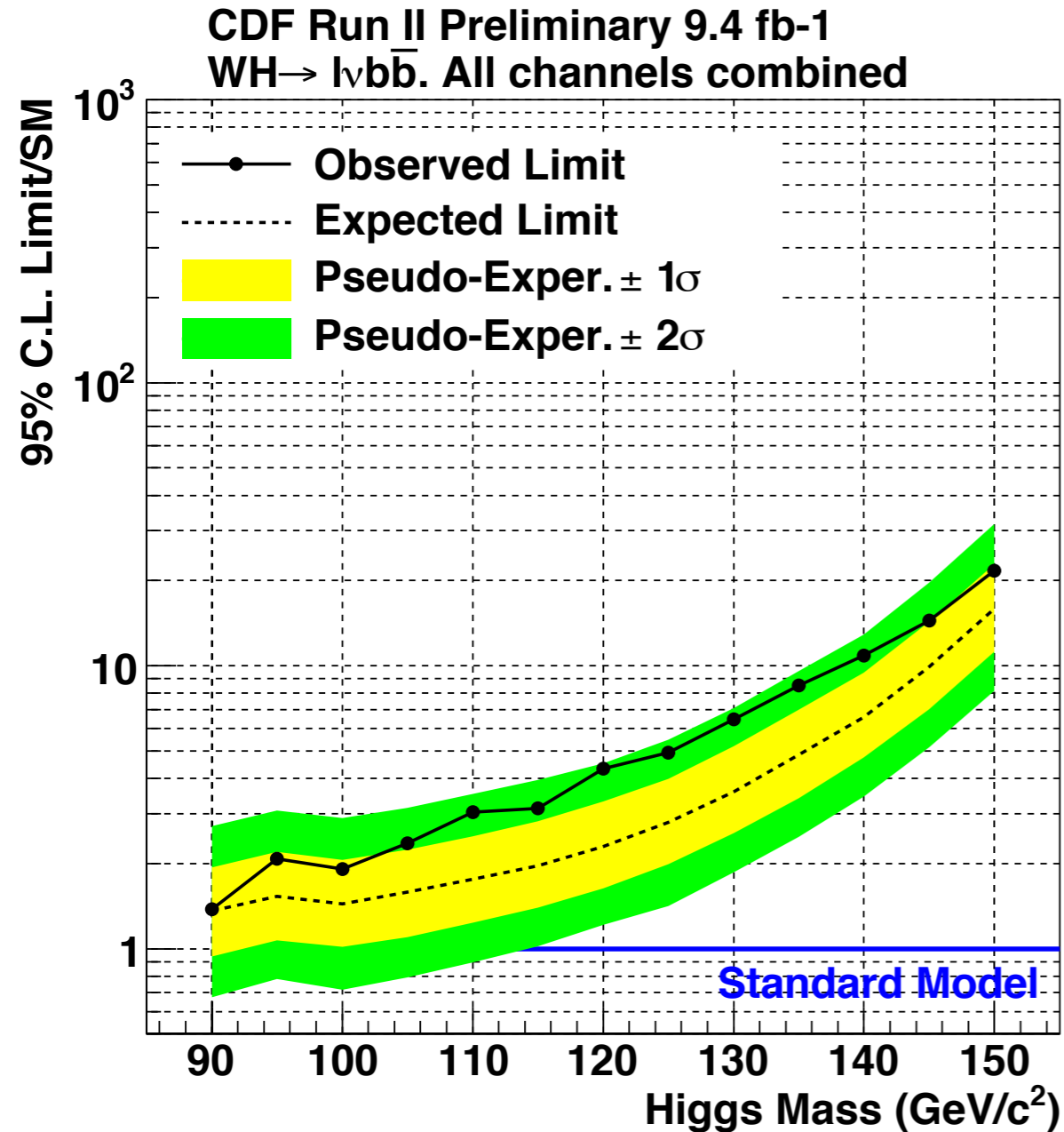
An Example Analysis: CDF $WH(\rightarrow l\nu b\bar{b})$

TABLE V: Systematic uncertainties for the CDF $l\nu b\bar{b}$ double tight tag (TT), one tight tag and one loose tag (TL) and double loose tag (LL) channels. Systematic uncertainties are listed by name; see the original references for a detailed explanation of their meaning and on how they are derived. Uncertainties are relative, in percent on the event yield. Shape uncertainties are labeled with an “(S)”.

CDF $l\nu b\bar{b}$ double tight tag (TT) channels relative uncertainties (%)						
Contribution	W+HF	Mistags	Top	Diboson	Non-W	WH
Luminosity ($\sigma_{\text{inel}}(p\bar{p})$)	3.8	0	3.8	3.8	0	3.8
Luminosity Monitor	4.4	0	4.4	4.4	0	4.4
Lepton ID	2.0-4.5	0	2.0-4.5	2.0-4.5	0	2.0-4.5
Jet Energy Scale	4.0-16.6(S)	0.9-3.3(S)	0.9-10.4(S)	4.7-19.7(S)	0	2.3-13.6(S)
Mistag Rate (tight)	0	40	0	0	0	0
Mistag Rate (loose)	0	0	0	0	0	0
B-Tag Efficiency (tight)	0	0	7.8	7.8	0	7.8
B-Tag Efficiency (loose)	0	0	0	0	0	0
$t\bar{t}$ Cross Section	0	0	10	0	0	0
Diboson Rate	0	0	0	6.0	0	0
Signal Cross Section	0	0	0	0	0	5
HF Fraction in W+jets	30	0	0	0	0	0
ISR+FSR+PDF	0	0	0	0	0	6.4-12.6
Q^2	4.0-8.8(S)	0.9-1.8(S)	0	0	0	0
QCD Rate	0	0	0	0	40	0

CDF $l\nu b\bar{b}$ one tight and one loose tag (TL) channels relative uncertainties (%)						
Contribution	W+HF	Mistags	Top	Diboson	Non-W	WH
Luminosity ($\sigma_{\text{inel}}(p\bar{p})$)	3.8	0	3.8	3.8	0	3.8
Luminosity Monitor	4.4	0	4.4	4.4	0	4.4
Lepton ID	2.0-4.5	0	2.0-4.5	2.0-4.5	0	2.0-4.5
Jet Energy Scale	3.9-12.4(S)	0.9-3.3(S)	1.4-11.5(S)	5.0-16.0(S)		2.5-16.1(S)
Mistag Rate (tight)	0	19	0	0	0	0
Mistag Rate (loose)	0	10	0	0	0	0
B-Tag Efficiency (tight)	0	0	3.9	3.9	0	3.9
B-Tag Efficiency (loose)	0	0	3.2	3.2	0	3.2
$t\bar{t}$ Cross Section	0	0	10	0	0	0
Diboson Rate	0	0	0	6.0	0	0
Signal Cross Section	0	0	0	0	0	5
HF Fraction in W+jets	30	0	0	0	0	0
ISR+FSR+PDF	0	0	0	0	0	3.3-10.3
Q^2	3.9-7.7(S)	0.9-1.9(S)	0	0	0	0
QCD Rate	0	0	0	0	40	0

An Example Analysis: CDF WH(\rightarrow lvbb)



VII. CONCLUSIONS

We have presented the results of a search for the standard model Higgs boson decaying to $b\bar{b}$, produced in association with a W boson decaying into a charged lepton and neutrino. We find that for the dataset corresponding to an integrated luminosity of 9.45 fb⁻¹, the data agree with the SM background predictions within the systematic uncertainties. However, a small broad excess for signal-like events is evident in the data ($\lesssim 2$ sigma). We set upper limits on the Higgs boson production cross section times the $b\bar{b}$ branching ratio. We find that the observed (expected) upper limits $\sigma(pp \rightarrow W^\pm H) \times \text{Br}(H \rightarrow b\bar{b})$ range from 1.38 (1.36) \times SM to 21.7 (15.9) \times SM for masses ranging from 90 GeV/ c^2 through 150 GeV/ c^2 with 5 GeV/ c^2 mass increments. For 115 GeV/ c^2 the upper limit is 3.13 (1.97).

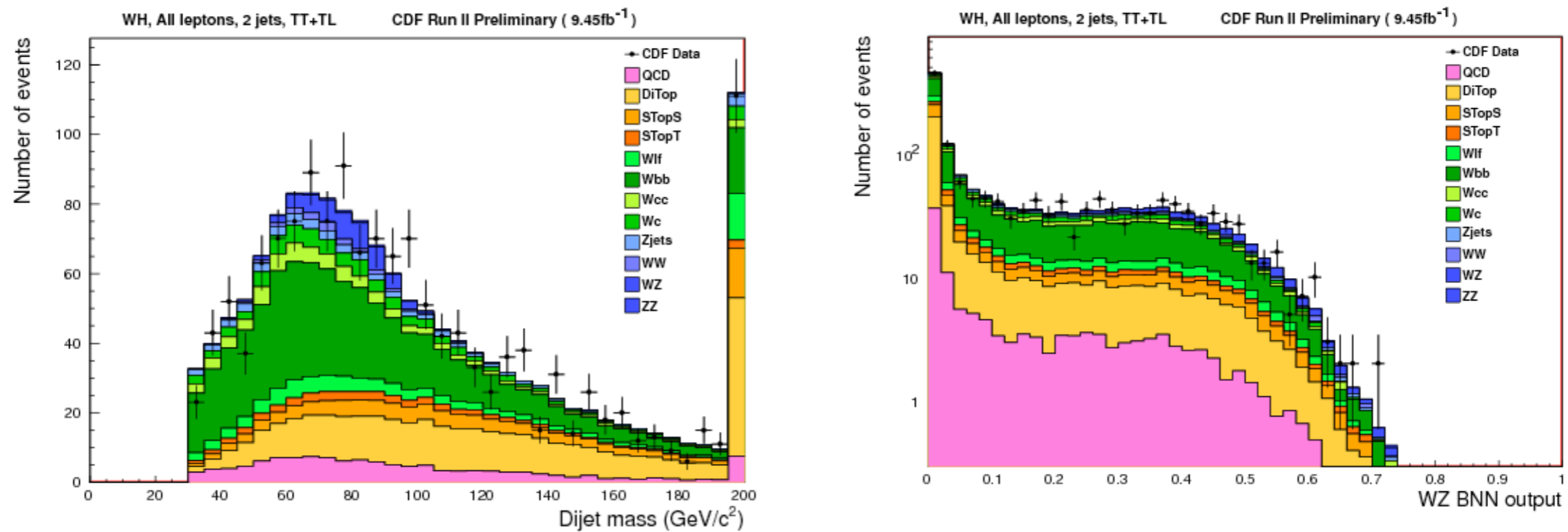
The increase in sensitivity over the previous 7.5 fb⁻¹ analysis [5] is $\sim 32\%$ at 115 GeV/ c^2 , out of which $\sim 11\%$ is due to the extra integrated luminosity and the rest of the gain is due to improved analysis techniques.

An Example Analysis: CDF WH(\rightarrow lvbb)

APPENDIX A: DIBOSON INTERPRETATION

The production of WZ boson pairs provides an important test of the electroweak sector of the standard model. In addition, the production rate is significantly higher than that for low-mass Higgs boson so a measurement of this process using the tools designed for the Higgs boson search could provide a powerful confirmation of the $WH \rightarrow \ell\nu b\bar{b}$ analysis. In $p\bar{p}$ collisions at $\sqrt{s} = 1.96$ TeV, the next-to-leading order (NLO) SM cross section for this process is $\sigma(WZ) = 3.2 \pm 0.2$ pb [21]. We perform the diboson analysis using exactly the same event selection and tools as are described above for the $WH \rightarrow \ell\nu b\bar{b}$ search.

The dijet mass distribution shown in Fig 1 is clearly sensitive to the diboson signal. However, in order to improve sensitivity and to validate the strategy used for $WH \rightarrow \ell\nu b\bar{b}$ we train a BNN to identify the WZ signal (see Fig 5).



We fit for the total WZ cross section distributions which yields $\sigma(WZ) = 5.63^{+1.79}_{-1.76}$ pb. We simultaneously fit all of the tag and lepton categories, but only use the two-jet events for this measurement. Fig. 6 shows the posterior

TABLE I. Luminosities, explored mass ranges, and references for the different processes and final states ($\ell = e$ or μ , and τ_{had} denotes a hadronic tau-lepton decay) for the CDF analyses. The generic labels “ $1 \times$,” “ $2 \times$,” “ $3 \times$,” and “ $4 \times$ ” refer to separations based on lepton or photon categories. The analyses are grouped in five categories, corresponding to the Higgs boson decay mode to which the analysis is most sensitive: $H \rightarrow b\bar{b}$, $H \rightarrow W^+W^-$, $H \rightarrow \tau^+\tau^-$, $H \rightarrow \gamma\gamma$, and $H \rightarrow ZZ$.

Channel		Luminosity (fb ⁻¹)	m_H range (GeV/ c^2)	Reference
$WH \rightarrow \ell \nu b\bar{b}$ 2-jet channels $4 \times$ ($5b$ -tag categories)		9.45	90–150	[42]
$WH \rightarrow \ell \nu b\bar{b}$ 3-jet channels $3 \times$ ($2b$ -tag categories)		9.45	90–150	[42]
$ZH \rightarrow \nu \bar{\nu} b\bar{b}$ ($3b$ -tag categories)		9.45	90–150	[43]
$ZH \rightarrow \ell^+ \ell^- b\bar{b}$ 2-jet channels $2 \times$ ($4b$ -tag categories)	$H \rightarrow b\bar{b}$	9.45	90–150	[44]
$ZH \rightarrow \ell^+ \ell^- b\bar{b}$ 3-jet channels $2 \times$ ($4b$ -tag categories)		9.45	90–150	[44]
$WH + ZH \rightarrow jjb\bar{b}$ ($2b$ -tag categories)		9.45	100–150	[45]
$t\bar{t}H \rightarrow W^+bW^- \bar{b}b\bar{b}$ (4 jets, 5 jets, ≥ 6 jets) \times ($5b$ -tag categories)		9.45	100–150	[46]
$H \rightarrow W^+W^-$ $2 \times$ (0 jets) + $2 \times$ (1 jet) + $1 \times$ (≥ 2 jets) + $1 \times$ (low- $m_{\ell\ell}$)		9.7	110–200	[47]
$H \rightarrow W^+W^-$ (e - τ_{had}) + (μ - τ_{had})		9.7	130–200	[47]
$WH \rightarrow WW^+W^-$ (same-sign leptons) + (trileptons)	$H \rightarrow W^+W^-$	9.7	110–200	[47]
$WH \rightarrow WW^+W^-$ (trileptons with 1 τ_{had})		9.7	130–200	[47]
$ZH \rightarrow ZW^+W^-$ (trileptons with 1 jet, ≥ 2 jets)		9.7	110–200	[47]
$H \rightarrow \tau^+\tau^-$ (1 jet) + (≥ 2 jets)	$H \rightarrow \tau^+\tau^-$	6.0	100–150	[48]
$H \rightarrow \gamma\gamma$ $1 \times$ (0 jet) + $1 \times$ (≥ 1 jet) + $3 \times$ (all jets)	$H \rightarrow \gamma\gamma$	10.0	100–150	[49]
$H \rightarrow ZZ$ (four leptons)	$H \rightarrow ZZ$	9.7	120–200	[50]

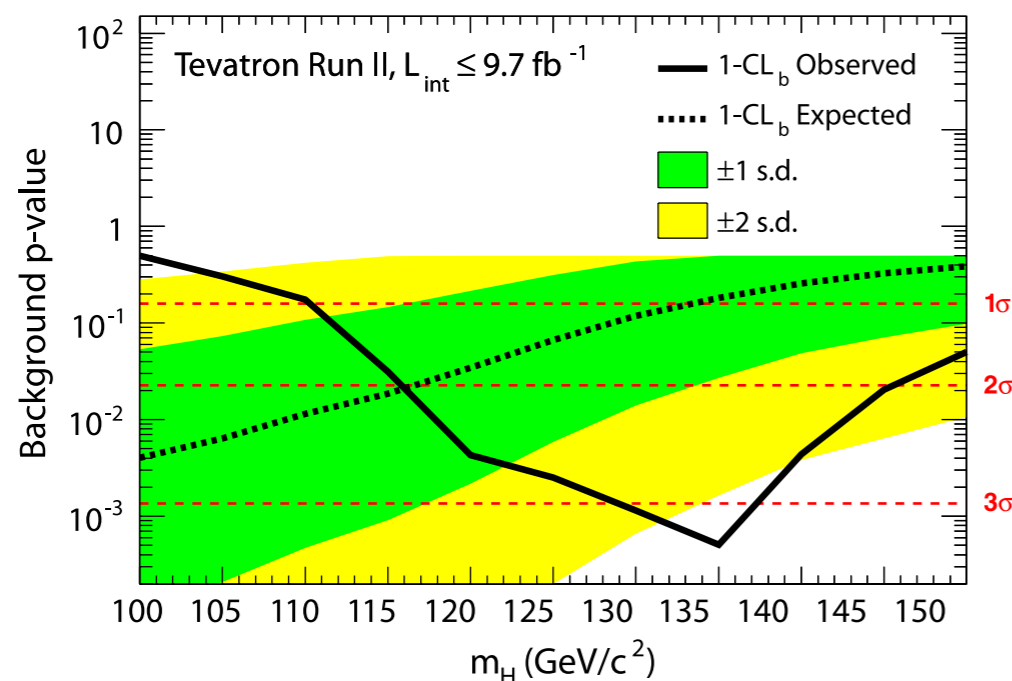
TABLE II. Luminosities, explored mass ranges, and references for the different processes and final states ($\ell = e$ or μ , and τ_{had} denotes a hadronic tau-lepton decay) for the D0 analyses. The generic labels “ $1 \times$,” “ $2 \times$,” “ $3 \times$,” and “ $4 \times$ ” refer to separations based on lepton, photon, or background characterization categories. The analyses are grouped in four categories, corresponding to the Higgs boson decay mode to which the analysis is most sensitive: $H \rightarrow b\bar{b}$, $H \rightarrow W^+W^-$, $H \rightarrow \tau^+\tau^-$, and $H \rightarrow \gamma\gamma$.

Channel		Luminosity (fb ⁻¹)	m_H range (GeV/ c^2)	Reference
$WH \rightarrow \ell \nu b\bar{b}$ 2-jet channels $2 \times$ ($4b$ -tag categories)		9.7	90–150	[51,52]
$WH \rightarrow \ell \nu b\bar{b}$ 3-jet channels $2 \times$ ($4b$ -tag categories)	$H \rightarrow b\bar{b}$	9.7	90–150	[51,52]
$ZH \rightarrow \nu \bar{\nu} b\bar{b}$ ($2b$ -tag categories)		9.5	100–150	[53]
$ZH \rightarrow \ell^+ \ell^- b\bar{b}$ $2 \times$ ($2b$ -tag) \times (4 lepton categories)		9.7	90–150	[54,55]
$H \rightarrow W^+W^- \rightarrow \ell^\pm \nu \ell^\mp \nu$ $2 \times$ (0 jets, 1 jet, ≥ 2 jets)		9.7	115–200	[56]
$H + X \rightarrow W^+W^- \rightarrow \mu^\mp \nu \tau_{\text{had}}^\pm \nu$ (3τ categories)		7.3	115–200	[57]
$H \rightarrow W^+W^- \rightarrow \ell \bar{\nu} jj$ $2 \times$ ($2b$ -tag categories) \times (2 jets, 3 jets)	$H \rightarrow W^+W^-$	9.7	100–200	[52]
$VH \rightarrow e^\pm \mu^\pm + X$		9.7	100–200	[58]
$VH \rightarrow \ell \ell \ell + X$ ($\mu\mu e$, $3 \times e\mu\mu$)		9.7	100–200	[58]
$VH \rightarrow \ell \bar{\nu} jjjj$ $2 \times$ (≥ 4 jets)		9.7	100–200	[52]
$VH \rightarrow \tau_{\text{had}} \tau_{\text{had}} \mu + X$ (3τ categories)	$H \rightarrow \tau^+\tau^-$	8.6	100–150	[58]
$H + X \rightarrow \ell^\pm \tau_{\text{had}}^\mp jj$ $2 \times$ (3τ categories)		9.7	105–150	[59]
$H \rightarrow \gamma\gamma$ (4 categories)	$H \rightarrow \gamma\gamma$	9.6	100–150	[60]



Evidence for a Particle Produced in Association with Weak Bosons and Decaying to a Bottom-Antibottom Quark Pair in Higgs Boson Searches at the Tevatron

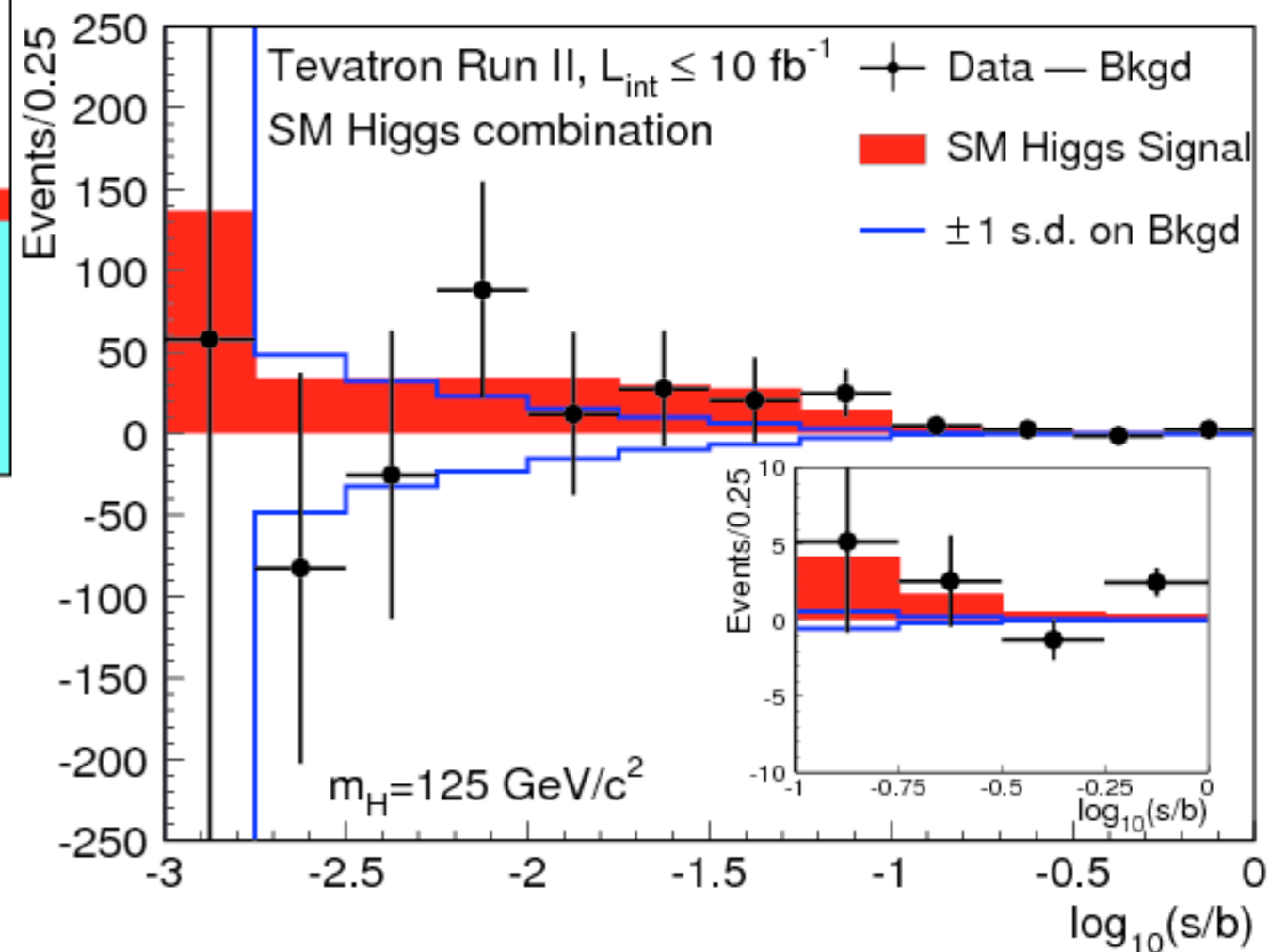
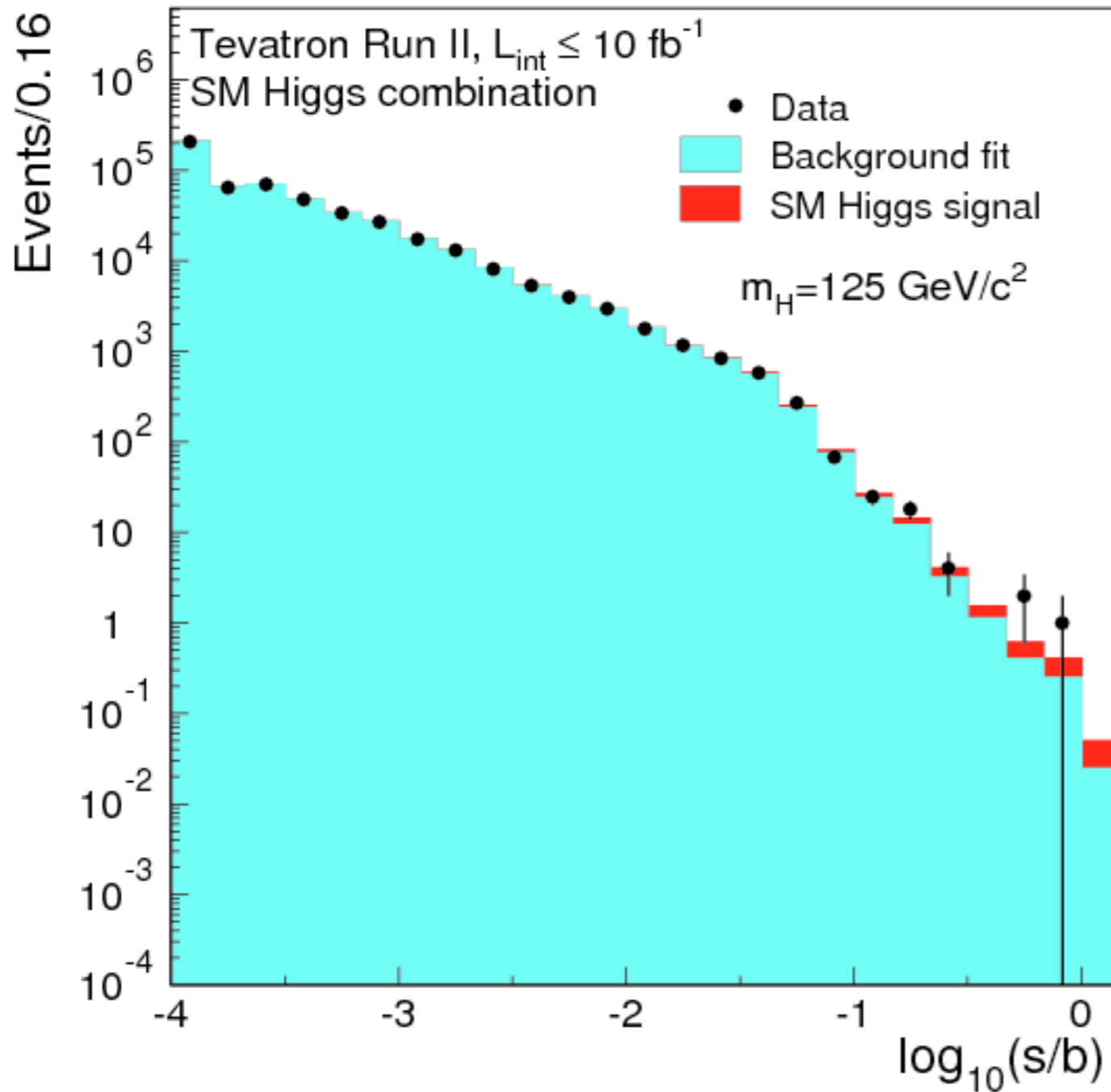
We combine searches by the CDF and D0 Collaborations for the associated production of a Higgs boson with a W or Z boson and subsequent decay of the Higgs boson to a bottom-antibottom quark pair. The data, originating from Fermilab Tevatron $p\bar{p}$ collisions at $\sqrt{s} = 1.96$ TeV, correspond to integrated luminosities of up to 9.7 fb^{-1} . The searches are conducted for a Higgs boson with mass in the range $100\text{--}150 \text{ GeV}/c^2$. We observe an excess of events in the data compared with the background predictions, which is most significant in the mass range between 120 and $135 \text{ GeV}/c^2$. The largest local significance is 3.3 standard deviations, corresponding to a global significance of 3.1 standard deviations. We interpret this as evidence for the presence of a new particle consistent with the standard model Higgs boson, which is produced in association with a weak vector boson and decays to a bottom-antibottom quark pair.



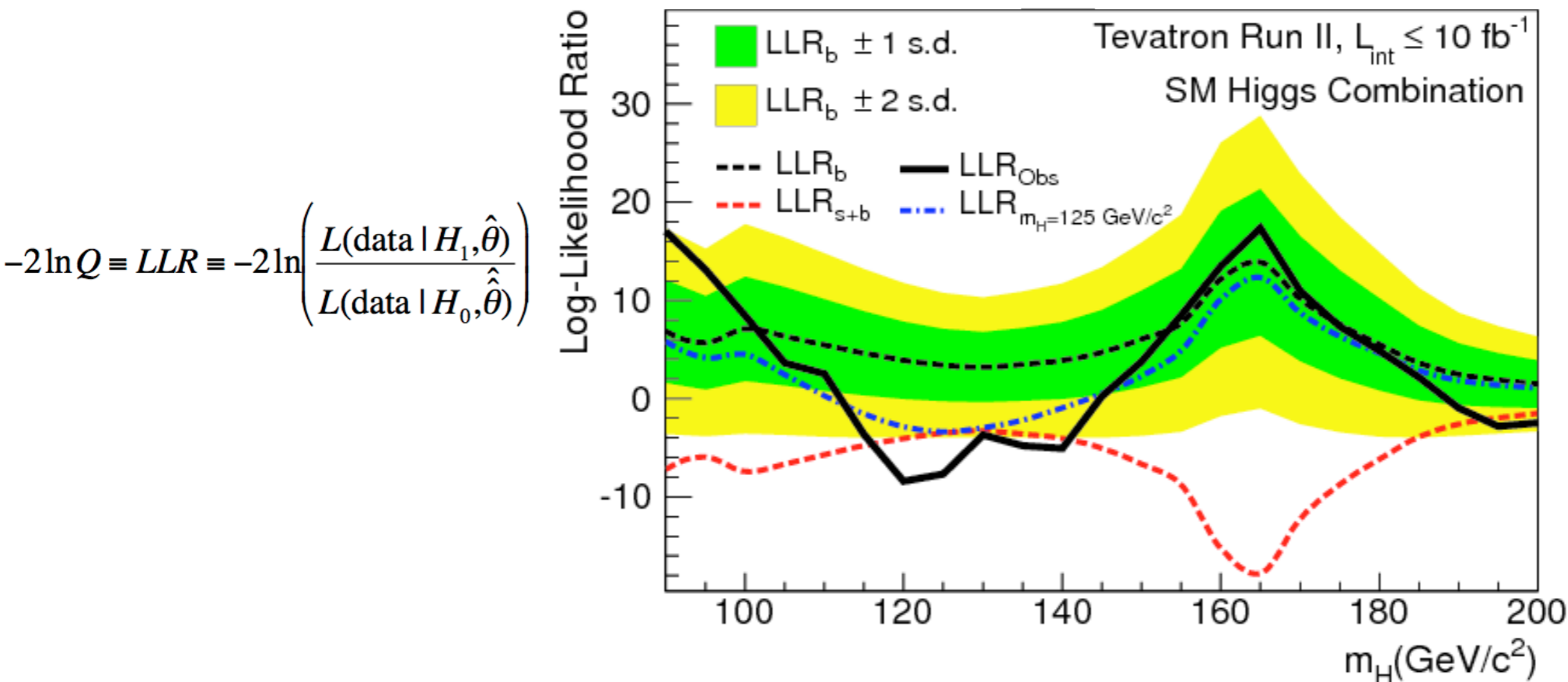
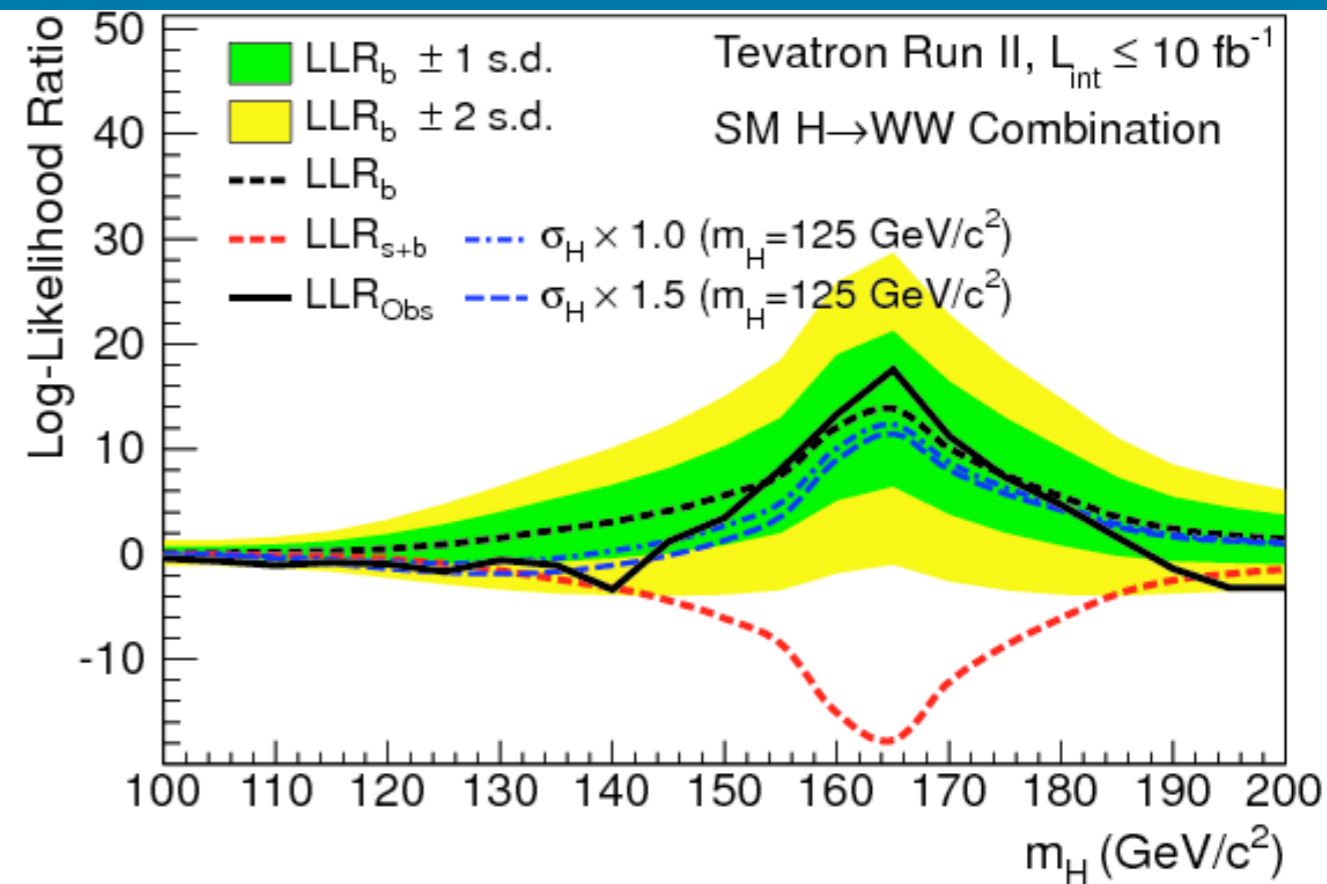
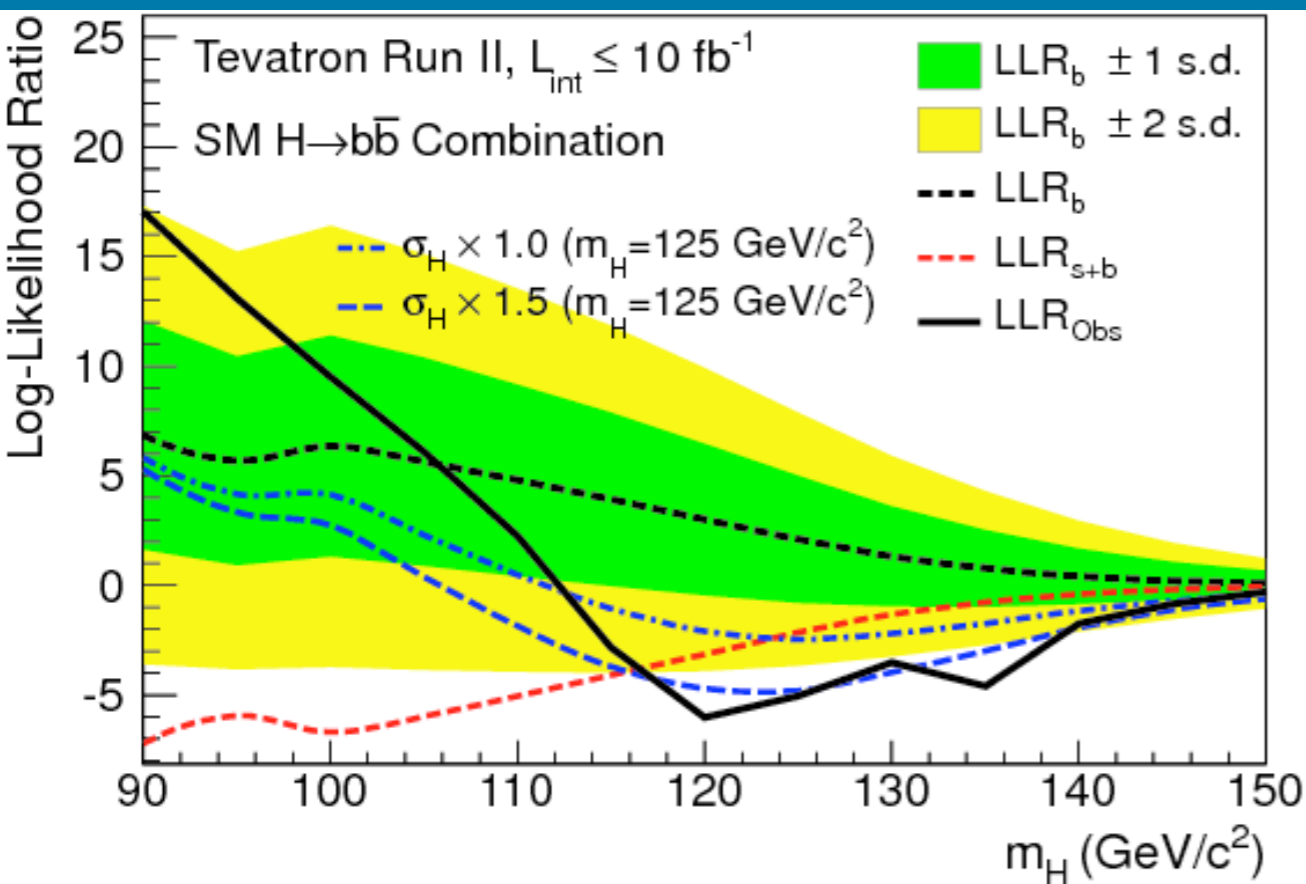
the exclusion limits for the SM Higgs boson mentioned earlier, there is no LEE and we derive a significance of 2.8 standard deviations for $m_H = 125 \text{ GeV}/c^2$.

We interpret this result as evidence for the presence of a particle that is produced in association with a W or Z boson and decays to a bottom-antibottom quark pair. The excess seen in the data is most significant in the mass range between 120 and $135 \text{ GeV}/c^2$, and is consistent with production of the SM Higgs boson within this mass range. Assuming a Higgs boson exists in this mass range, these results provide a direct probe of its coupling to b quarks.

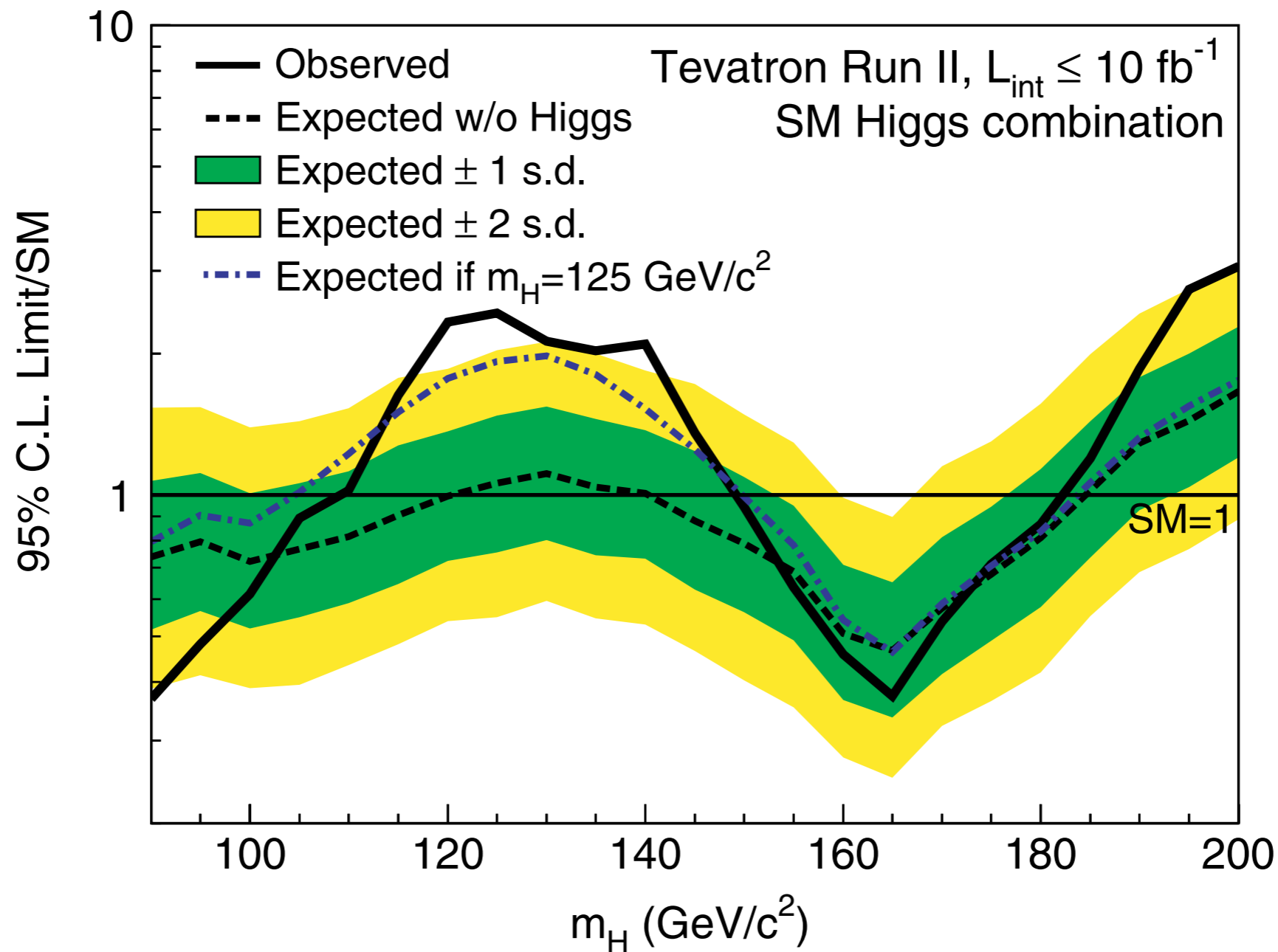
TeVatron Combination: Results



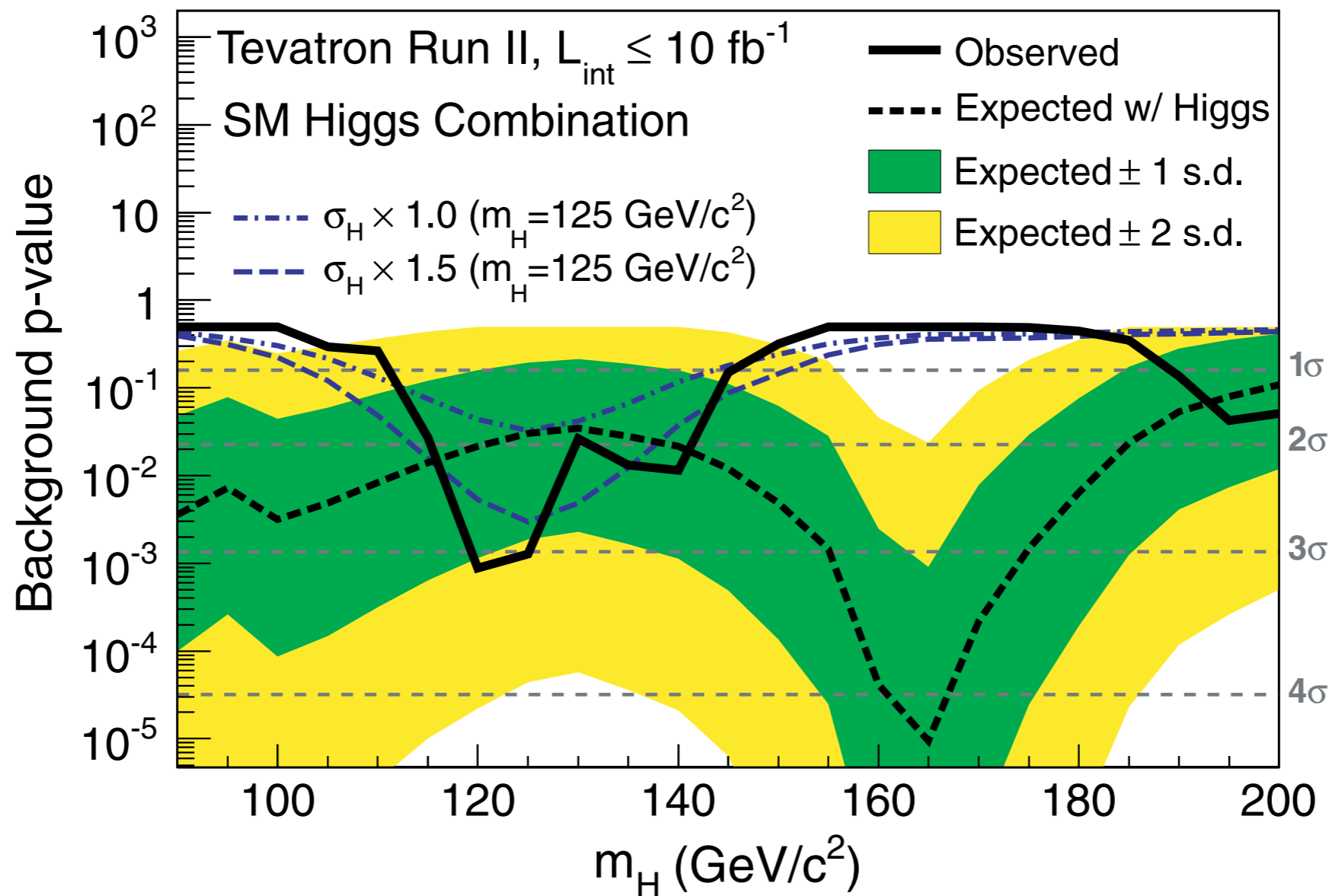
TeVatron Combination: LLR



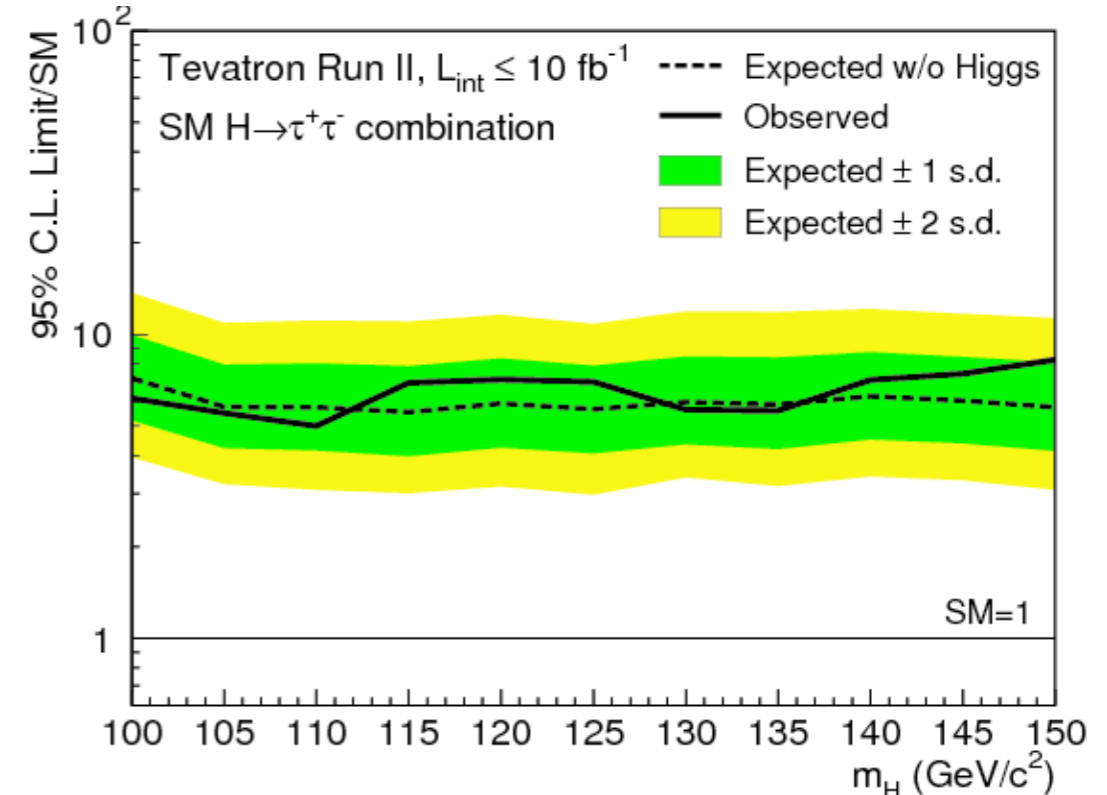
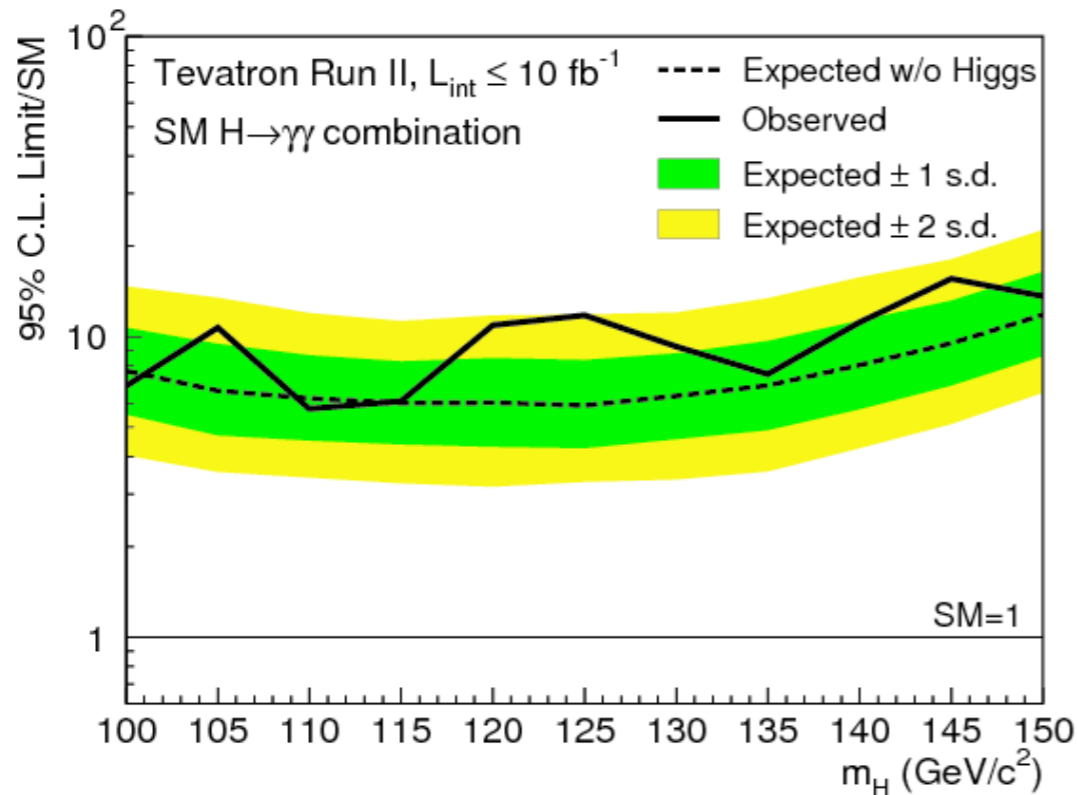
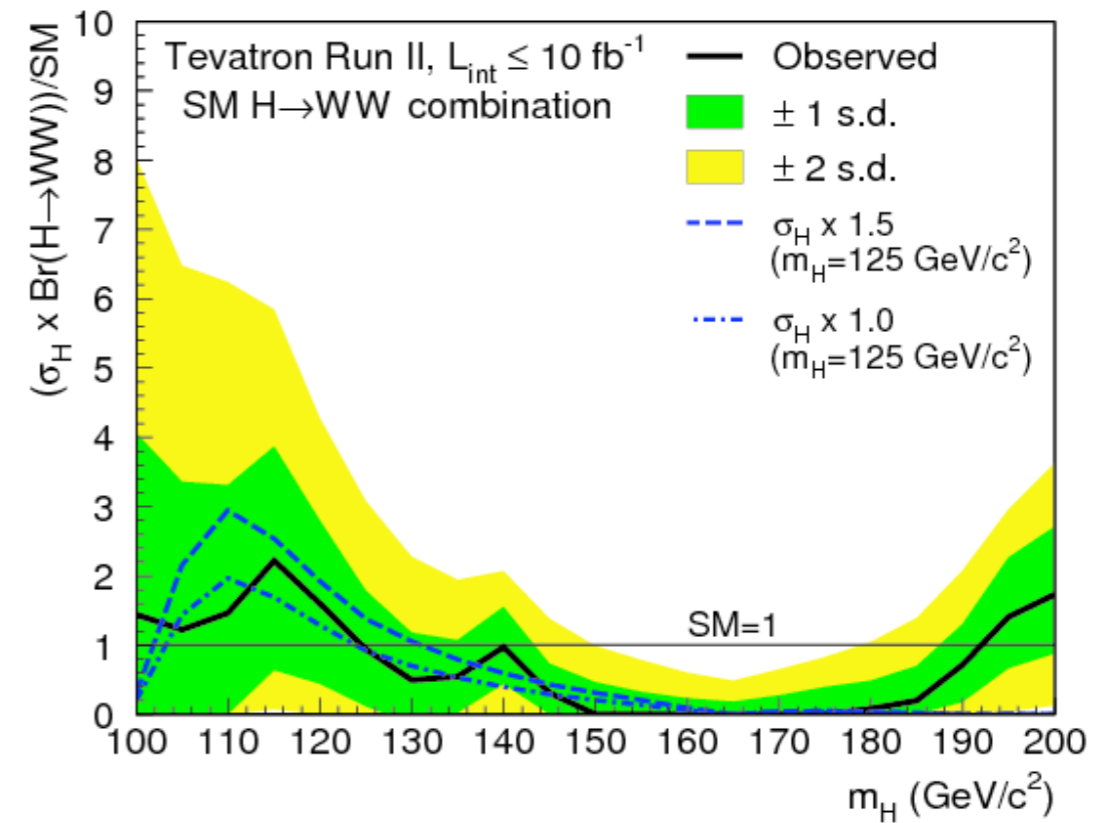
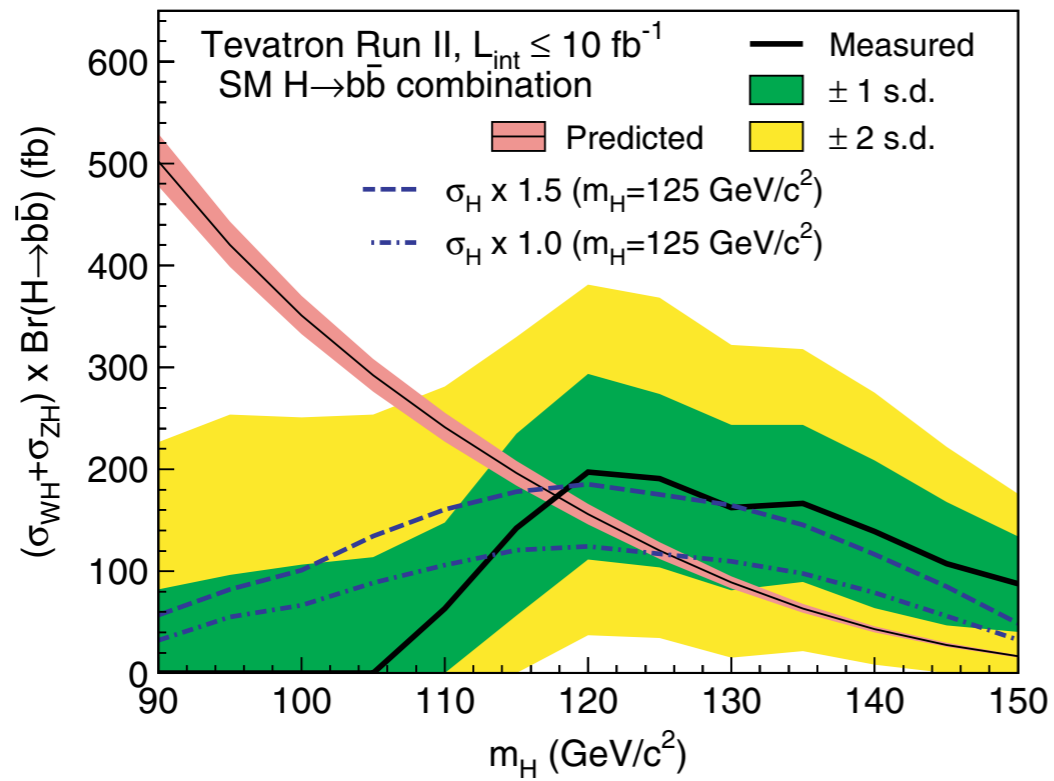
TeVatron Combination: Upper Limit



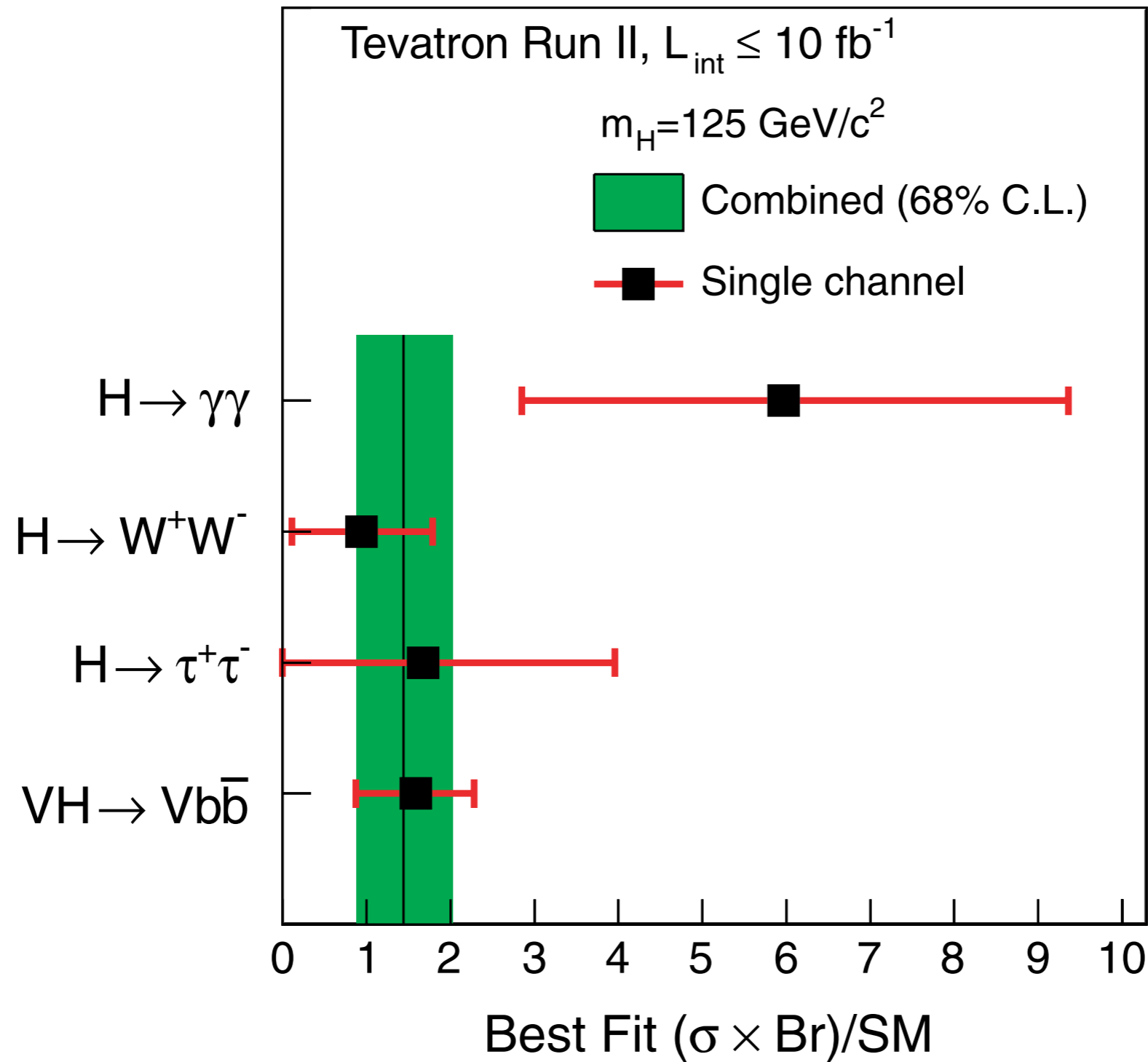
TeVatron Combination: p-value



TeVatron Combination: Best Fit Signal/Individual Limits



TeVatron Combination: Best Fit Signal Overview

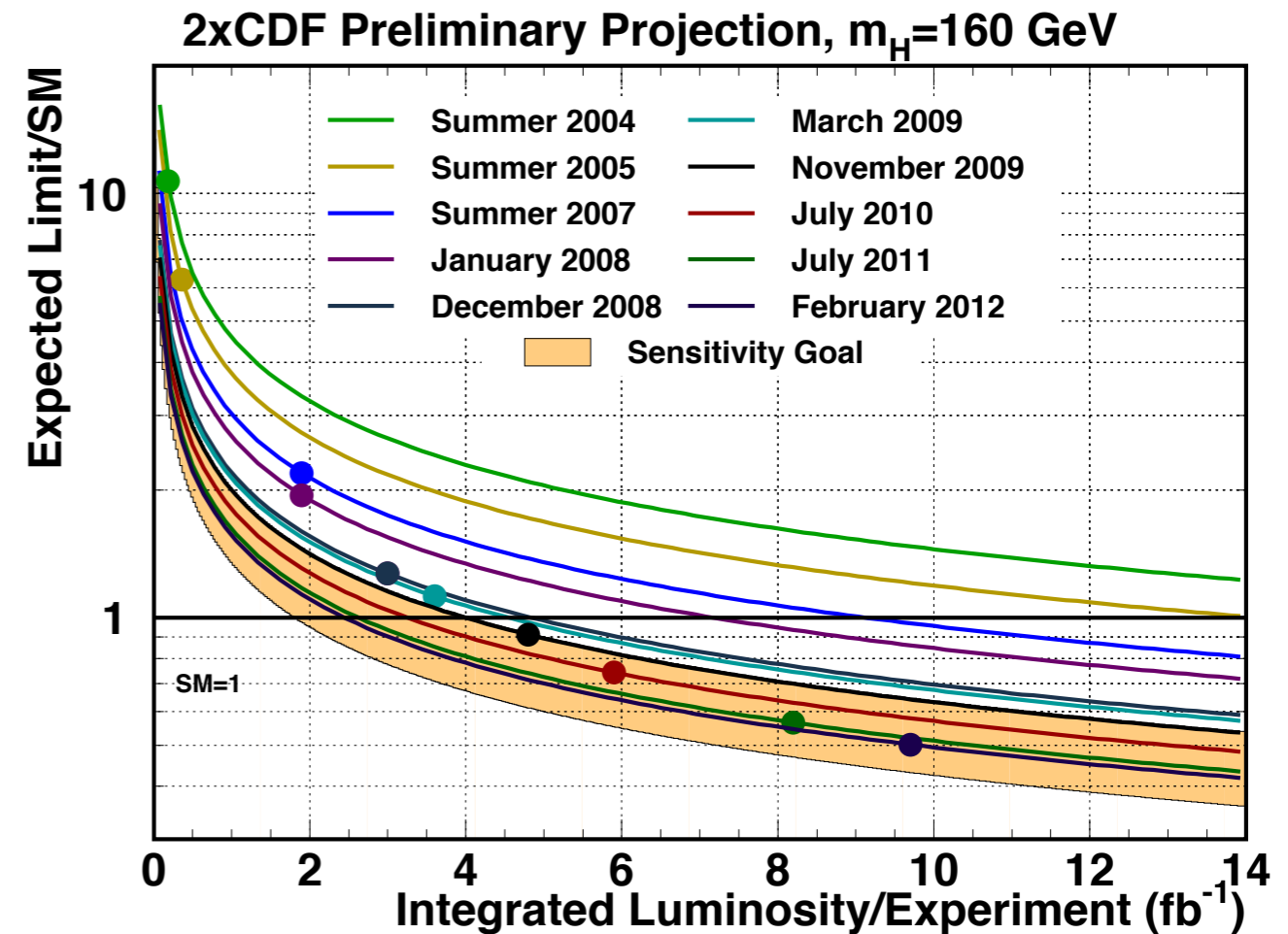
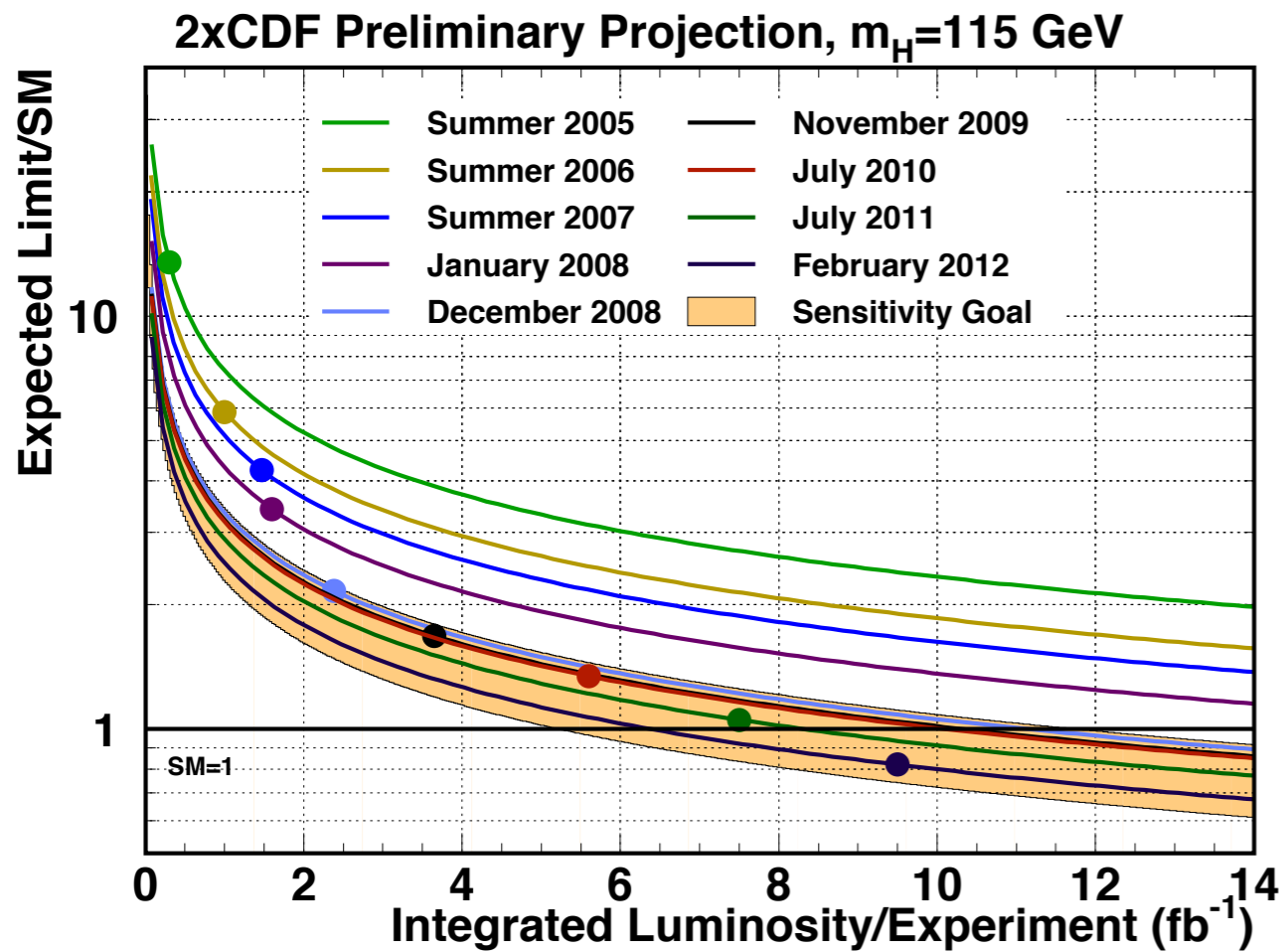


X. CONCLUSIONS

The search for the standard model Higgs boson at the Tevatron is challenging due to the small expected signal and the need to accurately model large background contributions. We have developed advanced tools to search for the Higgs boson in the leading production and decay modes predicted by the SM and control the impact of systematic uncertainties using constraints from the observed data. We have combined searches by the CDF and D0 Collaborations for the standard model Higgs boson in the mass range 90–200 GeV/ c^2 using Tevatron $p\bar{p}$ collision data corresponding to up to 10 fb $^{-1}$ of integrated luminosity collected at $\sqrt{s} = 1.96$ TeV. The results of searches focusing on the $H \rightarrow b\bar{b}$, $H \rightarrow W^+W^-$, $H \rightarrow ZZ$, $H \rightarrow \tau^+\tau^-$, and $H \rightarrow \gamma\gamma$ decay modes are included in the combination. The results are also interpreted in fermiophobic and fourth generation models. Fermiophobic Higgs bosons in the mass range 100–116 GeV/ c^2 are excluded at the 95% C.L., and a SM-like Higgs boson in the presence of a fourth sequential generation of fermions is excluded in the mass range 121–225 GeV/ c^2 at the 95% C.L. The SM Higgs boson is excluded, at the 95% C.L., from 90 to 109 GeV/ c^2 , and from 149 to 182 GeV/ c^2 . The expected exclusion regions in the absence of signal are 90–120 GeV/ c^2 and 140–184 GeV/ c^2 . The results of the $H \rightarrow b\bar{b}$ searches were validated through a measurement of the diboson ($WZ + ZZ$) production cross section using the same

data samples and analysis techniques, treating those diboson processes as signal. The resulting diboson cross-section measurement is in agreement with the SM prediction. We observe a significant excess of events in the mass range between 115 and 140 GeV/ c^2 . The local significance at $m_H = 125$ GeV/ c^2 corresponds to 3.0 standard deviations, with a median expected significance, assuming the SM Higgs boson is present at $m_H = 125$ GeV/ c^2 , of 1.9 standard deviations, with a best-fit signal strength of $1.44^{+0.59}_{-0.56}$ times the SM expectation. We also separately combined searches focusing on the $H \rightarrow b\bar{b}$, $H \rightarrow W^+W^-$, $H \rightarrow \tau^+\tau^-$, and $H \rightarrow \gamma\gamma$ decay modes. The observed best-fit signal strengths obtained from each of these combinations are consistent with the expectations for a SM Higgs boson at $m_H = 125$ GeV/ c^2 . We performed tests of the compatibility of the observed excess with the expectations for the couplings of a SM Higgs boson and saw no significant deviations.

TeVatron: Improvement beyond luminosity increase



Achieved and projected median expected upper limits on the SM Higgs boson cross section, by date.

The solid lines are $1/\sqrt{L}$ projections.

The top of the orange band corresponds to the Summer 2007 performance expected limit divided by 1.5, and the bottom of the orange band corresponds to the Summer 2007 performance expected limit divided by 2.25.

The luminosity for the March 2012 point is 9.5 fb^{-1} , a sensitivity-weighted average of the contributing channels' analyzed luminosities.

And this is the legacy of the TeVatron, not only discovered the top-quark and made several other observations and great measurements (m_t , m_W), but also the powerful multivariate techniques that have been developed and boosted the sensitivity of the analyses beyond what was thought to be feasible.

Additional Slides